Determination of Transport Parameters in Liquid Binary Electrolytes: Part II. Transference Number

Andreas Ehrl,[a,=,c] Johannes Landesfeind,[b,=,*,z] Wolfgang A. Wall,[a] and Hubert A. Gasteiger[b,]**

[a]*Institute for Computational Mechanics, Department of Mechanical Engineering, Technical University of Munich, Munich, Germany*
[b]*Chair of Technical Electrochemistry, Department of Chemistry and Catalysis Research Center, Technical University of Munich, Munich, Germany*

In the literature, various numerical methods for the simulation of ion-transport in concentrated binary electrolytes for lithium ion batteries can be found, whereas the corresponding transport parameters are rarely discussed. In this contribution, a novel method for the determination of the transference number in non-aqueous electrolytes is proposed. The method is based on data from a concentration cell and on the value of the thermodynamic factor obtained from independent measurements based on quantifying the redox potential of ferrocene. The concentration dependent transference numbers obtained by this new method are compared to values obtained by the classical approach, which is based on experiments in a polarization cell and a concentration cell. For the latter, a set of commonly used and some newly proposed analysis methods as well as their theoretical justification are discussed. Using an exemplary electrolyte (lithium perchlorate in a mixture of ethylene carbonate and diethyl carbonate), we will demonstrate that our newly proposed method based on concentration cell experiments and a thermodynamic factor derived from independent measurements is a more accurate approach for obtaining concentration dependent transference numbers. At the end, the experimentally determined concentration dependent transference numbers are compared to data available in the literature.

Manuscript submitted June 9, 2017; revised manuscript received August 8, 2017. Published September 9, 2017.

Numerical simulations are based on four different concentration dependent transport parameters, namely the conductivity $\kappa(c)$, the binary diffusion coefficient $D_{\pm}(c)$, the transference number $t_+(c)$, and the thermodynamic factor (TDF) or the mean molar activity coefficient $f_{\pm}(c)$, respectively. The accurate determination of these parameters is key for the reliable simulation of the charge/discharge performance of lithium ion batteries. The conductivity $\kappa(c)$, the binary diffusion coefficient $D_{\pm}(c)$,[1] and the thermodynamic factor[2] can be determined by a single experiment for each concentration. The determination of the concentration dependent transference number is more elaborate. In the following, an overview of various experimental techniques for the determination of transference numbers in lithium based electrolytes is given. In the context of this work the term transference number is used as defined in Newman and Thomas-Alyea.[3]

The transference number $t_+(c)$ can be determined directly by the Hittorf method which is discussed for polymer electrolyte solutions by Bruce et al.[4] An alternative version of the Hittorf method for liquid electrolytes was applied by Valøen and Reimers for $LiPF_6$ in PC:EC:DMC (10:27:63 v:v:v).[5] Since the influence of diffusion processes on mass transport is neglected in the derivation of the Hittorf method,[5] it can be not used for an accurate determination of the transference number in general. Additionally, the noise level observed with the Hittorf method as reported by Valøen and Reimers is too large for the determination of the transference number as a function of the concentration.[5] On the other hand, for dilute electrolyte solutions, the potentiostatic polarization method introduced in Bruce and Vincent[6] can be used for the direct determination of the transference number. In this work, as well as in Hiller et al.,[7] the method is used for polymer electrolytes, while Mauro et al.[8] and Zugmann et al.[9] applied the same method for liquid electrolytes such as $LiClO_4$ dissolved in PC and for $LiPF_6$ in various solvents, albeit at concentrations which cannot anymore be considered as dilute electrolytes. In Zugmann et al., three additional methods, namely the electromotive force method, the NMR method, and the galvanostatic polarization method are discussed.[9] The electromotive method is based on data from a concentration cell with transference,[10] including concentration overpotentials. In such an experimental setup, the transference number can be determined either in the dilute electrolyte limit,[5] where the thermodynamic factor can be assumed to be unity,[3] or the functional dependence of the thermodynamic factor on salt concentration has to be known or assumed. It would also be possible to use a concentration cell without transference,[10] but it is difficult to find appropriate salt bridges for aprotic lithium based electrolytes, which would satisfy the condition $t_+ = t_- = 0.5$.[9] The transference number can also be determined by measuring the ionic self-diffusion coefficients.[11,12] In Zhao et al.,[13] the method introduced by Bruce and Vincent[6] is compared to the NMR method, revealing that completely different values for the transference number are obtained, even for the smallest concentrations. In Sethurajan et al., the differences between transference numbers determined by NMR and other techniques are explained by the effect of ion-pairing.[14] In their publication, it is strictly distinguished between the transference number which is defined based on a current fraction versus the transport number which is defined based on the ionic diffusion coefficients. In the absence of ion-pairs, both definitions are equivalent, as can be concluded from the derivation of concentrated solution theory presented in Newman and Thomas-Alyea.[3] The most popular method to determine the transference number is the galvanostatic polarization method. It is used for polymer electrolytes in Ma et al.,[15] Ferry et al.[16] or Doeff et al.[17] However, the determination of the transference number by the galvanostatic polarization requires knowledge about the diffusion coefficient and thermodynamic factor. Therefore, it is necessary to perform three different experiments to determine the transference number, which usually results in an accumulation of inaccuracies from the errors in each experimental procedure and due to the necessity to use arbitrary functional relationships (e.g., assuming a concentration independent transference number in some cases). Alternatively, the diffusion coefficient, the transference number, and the thermodynamic factor can also be determined by a numerical optimization approach as shown in the publications by Georén and Lindbergh,[18] Nyman et al.,[19] and Lundgren et al.[20] In this approach, usually, the same or similar experiments as for the galvanostatic polarization are performed.

=These authors contributed equally to this work.
*Electrochemical Society Student Member.
**Electrochemical Society Fellow.
[c]Present address: Velling 4, 94374 Schwarzach, Germany.
[z]E-mail: j.landesfeind@tum.de

In the following, various of the aforementioned electrochemical methods for the determination of the transference number are reviewed regarding theoretical assumptions, experimental accuracy, and applicability. Additionally, an alternative method for the determination of the transference number based on the combination of measuring the redox potential of ferrocene/ferrocenium vs. lithium salt concentration[2] and a concentration cell is introduced. All discussed methods are also investigated experimentally before the final conclusion is presented. After presentation of the used materials and measurement setups in the Experimental section, the relevant theoretical framework is discussed in the Theory section, summarizing the equations used for the determination of the transference number used in the literature as well as newly introduced analysis methods. Validity and accuracy of the introduced techniques are analyzed and compared in the Numerical Validation section. Because theoretically expected transients are more obvious in simulated experiments, this section aids in understanding experimental data. In the Results and discussion section, the transference number is obtained from measurements in previously described cell setups. A short summary and a conclusion are given in the Conclusions.

Experimental

Ethylene carbonate (EC, 50%, by weight, Sigma Aldrich, anhydrous, 99%) and diethyl carbonate (DEC, 50%, by weight, Sigma Aldrich, anhydrous, >99%) were used as solvents for self-prepared electrolytes containing lithium perchlorate ($LiClO_4$, Sigma Aldrich, 99.99%) salt, whereby all components were mixed in an argon filled and temperature controlled glove box (MBraun, 25°C ± 1°C, water content <0.1 ppm, Ar 5.0, Westfalen, 99.999% vol). $LiClO_4$ concentrations ranged from 0.1×10^{-3} to 2 M. Metallic lithium (Rockwood Lithium, 0.45 mm, high purity) was used as counter electrode (CE) and working electrode (WE).

In this contribution, a polarization and a concentration cell are used for the determination of transference numbers. The polarization cell consists of two parallel and aligned lithium electrodes which are separated by porous separators, as described in detail in part I of this publication, where we presented the determination of diffusion coefficients.[1] The concentration cell consists of two parallel lithium stripes which are in contact with a stripe of glass fiber separator soaked with two electrolyte solutions which differ in their lithium salt concentration. To minimize electrolyte evaporation, separator and electrodes are sandwiched between two glass plates as depicted in Figure 1. Concentration cell potentials were measured over a time interval of four minutes using either a handheld voltmeter (Voltcraft VC830) inside the glove box or a potentiostat (Biologic VMP3).

Theory

In the following, the theoretical foundations of various methods for the determination of the transference number are discussed. First, the direct determination of the transference number for dilute electrolytes introduced by Bruce and Vincent[6] is embedded into the concentrated solution theory. Afterwards, the classical method for the determination of the transference number in concentrated electrolytes based on measurements in a polarization and concentration cell is shortly reviewed. A basic element of this method is the Sand equation. In the following, the same experimental setup is used to determine the transference number, but the Sand equation is replaced by several alternative analytical relations, which so far have not been used for the determination of the transference number. In the end of this section, a novel method for the determination of the transference number in concentrated electrolytes is introduced, which is based on measurements in a concentration cell and which makes use of the quantification of the thermodynamic factor in an independent experiment[2] based on measuring the redox potential of ferrocene/ferrocenium vs. lithium salt concentration (further on referred to as "ferrocene cell").

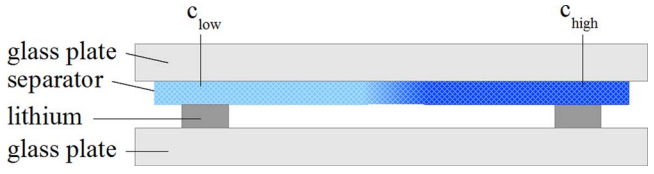

Figure 1. Concentration cell setup for the determination of concentration overpotentials between two lithium electrodes contacted by a glass fiber separator soaked with an electrolyte of two different salt concentrations (side view).

Direct determination of the transference number by steady-state polarization experiments.—The direct determination of the transference number t_+ for dilute electrolyte solutions is based on the application of a constant cell potential U_p until the steady-state current is reached. Theoretically, it is possible to calculate the transference number t_+ from the ratio between the initial current I_0 and the steady-state current I_s. However, a correction term for variable electrode kinetics as a result of, e.g., the SEI formation or the growth of mossy lithium has to be considered. In the original form introduced by Blonsky et al., the method was restricted to dilute electrolyte solutions with a constant diffusion coefficient.[21] Bruce and Vincent[6] extended it to electrolyte solutions with a variable ionic diffusion coefficient. In this extension, it is argued that the thermodynamic factor has to be close to unity in order to apply the dilute solution theory. However, it is also possible to derive the method from the more general framework of concentrated electrolyte solutions as discussed, e.g., in Doyle[22] and Ehrl.,[23] which is outlined in the following (Eq. 1 to 24). Comparison of the result obtained using this approach with the Bruce-Vincent equation will allow to obtain a mathematical condition which has to be fulfilled for the dilute solution theory to be applicable. The potential difference $\Delta\Phi$ between the anode A and the cathode C for a one-dimensional approximation of an electrochemical cell is given by the integration of Eq. 3 in part I of this publication (Ref. 1).

$$\Delta\Phi = I \int_C^A \left(\frac{1}{\kappa\,(c_0)} \frac{l}{A} \frac{\tau}{\varepsilon} \right) \mathrm{d}x \; + \frac{\nu}{\nu_+ z_+} \frac{\mathrm{RT}}{\mathrm{F}} \left[1 + \frac{\partial \ln f_\pm\,(c_0)}{\partial \ln c} \right] \cdot (1 - t_+\,(c_0)) \frac{\Delta c}{\mathrm{c_0}} \qquad [1]$$

The potential difference $\Delta\Phi$ denotes the volumetric intrinsic phase average of the electric potential, I the current, A the electrode area, l the distance between the electrodes, and c_0 the initial volumetric intrinsic phase average of the concentration.[1] The porosity ε and the tortuosity τ are parameters related to the morphology of the porous medium and are frequently used, e.g., to obtain the so-called effective binary diffusion coefficient $D_{\pm,\mathrm{eff}} = \varepsilon\,\tau^{-1}\,D_\pm$ or the effective conductivity $\kappa_{\mathrm{eff}} = \varepsilon\,\tau^{-1}\,\kappa_{\mathrm{eff}}$. While porosities can be measured gravimetrically the tortuosity of porous media may be determined from impedance measurements in symmetric cells.[24] The conductivity $\kappa(c_0)$, the transference number $t_+(c_0)$, and the thermodynamic factor $\left[1 + \frac{\partial \ln f_\pm(c_0)}{\partial \ln c}\right]$ are the first order approximations of the concentration dependent conductivity $\kappa(c)$, the transference number $t_+(c)$, and the thermodynamic factor $\left[1 + \frac{\partial \ln f_\pm(c)}{\partial \ln c}\right]$.[1] The coefficient $\nu = \nu_+ + \nu_-$ is based on the stoichiometry coefficients ν_+ and ν_- resulting from the dissociation of a binary salt in its components (e.g., $\nu = 2$ for the typical 1:1 salts used in lithium ion batteries). The gas constant is denoted by R (8.314 J/(mol K)), the Faraday constant (96485 As/mol) by F, and the temperature by T (in units of Kelvin).

In contrast to Eq. 8 in part I of this publication (Ref. 1) which is only valid in the absence of current flow, an additional ohmic contribution, accounting for the current flow through the cell, has to be considered for the potential difference $\Delta\Phi$. The integral in Eq. 1 is equivalent to the ohmic resistance R_{el} of the electrolyte solution. Therefore, the initial potential difference $\Delta\Phi_0$ during the polarization reads

$$\Delta\,\Phi_0 = R_{\mathrm{el},0}\;\; I_0 \qquad [2]$$

since the concentration difference Δc is very small directly after the application of the cell potential U_p. The initial electrolyte resistance

is denoted by $R_{el,0}$. At the steady-state, the potential difference $\Delta\Phi_s$ is given by

$$\Delta\Phi_s = R_{el,s} I_s + \frac{\nu}{\nu_+ z_+} \frac{RT}{F} \left[1 + \frac{\partial \ln f_\pm(c_0)}{\partial \ln c}\right] (1 - t_+(c_0)) \frac{\Delta c_s}{c_0} \quad [3]$$

The initial and the steady-state electrolyte resistance measured by impedance spectroscopy (high frequency resistance) can be assumed to be identical

$$R_{el,0} = R_{el,s} = R_{el} \quad [4]$$

since the variation of the conductivity is negligible for small concentration variations. It is also assumed that the concentration difference Δc_S between the electrodes follows a linear concentration profile at steady-state. Due to the known concentration profile, Eq. 6 in part I of the publication (Ref. 1) can be used to express the concentration difference between anode and cathode.

$$\Delta c_S = c(T_I) = \frac{1}{z_+ \nu_+ F} \frac{1 - t_+(c_0)}{D_{\pm,eff}(c_0)} \frac{l}{A} I_s \quad [5]$$

In a next step, Eqs. 2 and 3 can be inserted into Eq. 4 and combined with Eq. 5 giving the following equation

$$\frac{I_0\,\Delta\Phi_s}{I_s\,\Delta\Phi_0} = 1 + \frac{\nu}{\nu_+^2 z_+^2} \frac{R\,T}{F^2} \left[1 + \frac{\partial \ln f_\pm(c_0)}{\partial \ln c}\right] \frac{(1 - t_+(c_0))^2}{D_{\pm,eff}(c_0)} \cdot \frac{l}{A\,c_0\,R_{el,0}} \quad [6]$$

Eq. 6 simplifies to the following equation for dilute electrolyte solutions

$$t_+ = \frac{I_s\,\Delta\Phi_0}{I_0\,\Delta\Phi_s} \quad [7]$$

if the following approximations are made according to the dilute solution theory

$$1 + \frac{\partial \ln f_\pm(c_0)}{\partial \ln c} \approx 1 \quad [8]$$

$$\kappa_- \approx \frac{F^2}{R\,T} z_-^2\,\nu_-\,D_-\,c_0 \quad [9]$$

in combination with the definitions for a binary electrolyte

$$(1 - t_+) \equiv t_- \quad [10]$$

$$\frac{\kappa_{eff}}{D_{\pm,eff}} \equiv \frac{\kappa}{D_\pm} \quad [11]$$

$$t_- \equiv \frac{\kappa_-}{\kappa} \quad [12]$$

$$D_\pm \equiv \frac{(z_+ - z_-)\,D_+\,D_-}{D_+ + D_-} \quad [13]$$

$$t_+ = \frac{z_+ D_+}{z_+ D_+ - z_- D_-} \quad [14]$$

Here, κ_- is the anion contribution to the ionic conductivity and D_+/D_- are the diffusion coefficients of the cation/anion.

An alternative formulation of Eq. 7 can be found

$$t_+ = \frac{I_s\,\left(U_p - \left(R_{LF,0} - R_{el,0}\right) I_0\right)}{I_0\left(U_p - \left(R_{LF,s} - R_{el,s}\right) I_s\right)} = \frac{I_s\,\left(U_p - \left(R_{LF,0} - R_{el}\right) I_0\right)}{I_0\left(U_p - \left(R_{LF,s} - R_{el}\right) I_s\right)} \quad [15]$$

if the initial $\Delta\Phi_0$ (see Eq. 2) and steady-state potential difference $\Delta\Phi_s$ (see Eq. 3) are replaced by the following relation

$$\Delta\,\Phi_i = U_p - \left(R_{LF,i} - R_{el,i}\right) I_i \quad [16]$$

and if the assumption of a constant electrolyte resistance given in Eq. 4 is used. Here, R_{LF} denotes the low frequency (LF) resistance determined by impedance spectroscopy. The low-frequency resistance is the overall resistance of a serial equivalent circuit consisting of the electrolyte resistance R_{el} and additional resistances such as kinetic resistances or contact resistances. The subscript s indicates the steady state and 0 the initial state. Due to small concentration variations, the initial and steady-state electrolyte resistances $R_{el,s} = R_{el,0}$ can be assumed to be equal as indicated already in the beginning of the derivation. A similar formulation as given in Eq. 15 was introduced by Bruce and Vincent.[6]

The comparison of Eq. 6 and Eq. 7 gives a mathematical condition for the validity of the dilute solution theory and the corresponding transport parameter:

$$\underbrace{t_+ + t_-}_{=1} \left[\underbrace{\frac{\nu}{\nu_+^2 z_+^2} \frac{R\,T}{F^2} \left(1 + \frac{\partial \ln f_\pm(c_0)}{\partial \ln c}\right) \frac{t_+(c_0)(1 - t_+(c_0))}{D_\pm(c_0)} \frac{\kappa(c_0)}{c_0}}_{=1}\right] = 1 \quad [17]$$

The expression in the brackets has to be equal to one for the dilute solution theory to be applicable, since by definition the sum of the transference numbers t_+ and t_- is one.

Considering that the initial low frequency resistance corresponds to $R_{LF,0} = U_p / I_0$, and combining this with Eq. 4, allows a simplification of Eq. 15 to

$$t_+(c_0) = \frac{I_s\,R_{el}}{U_p - \left(R_{LF,s} - R_{el}\right) I_s} \quad [18]$$

which was introduced by Hiller et al.[7] The advantage of this formulation is that the number of parameters which has to be determined is reduced compared to Eq. 15. In addition, the steady-state current I_s is much easier to determine than the initial current I_0, which may include additional effects such as double layer charging and a non-uniform interface resistance.

The determination of the initial current I_0 can be improved by extrapolation of the initial time behavior of the current back to the start of the polarization. The theoretical time behavior of the current $I(t)$ in such an experiment can be derived from the partial differential equation of the form

$$\frac{\partial c}{\partial t} - D^*_{\pm,eff}(c_0)\,\nabla^2 c = 0, \text{ in } (0, l) \times (0, T_I) \quad [19]$$

with the current I as boundary condition (BC) at anode and cathode. This scalar transport equation results from the ion-transport equations given in part I of this publication (Ref. 1) by applying the one-dimensional approximation for the ion-transport equations (compare Ref. 1). The semi-infinite limit

$$\lim_{x \to \infty} c = c_0 \quad [20]$$

is used as an additional condition and can be interpreted as $c \to c_0$ for $x \to l/2$, which introduces a limitation for the time range in which the analytical solution is valid. A uniform concentration profile is assumed as an initial condition. This boundary value problem can be solved by Laplace transformation as shown in, e.g., Bard and Faulkner[25] (Responses based on linear diffusion and a planar electrode, chapter 5.5.1) or Ehrl.[23] As a result, the current $I(t)$ at the anode as well as the cathode can be expressed as

$$I(t) = \frac{U_p}{R_{LF,0}} \exp\left(H^2 t\right) \operatorname{erfc}\left(H\,t^{1/2}\right) \quad [21]$$

where $\mathrm{erfc}(H\sqrt{t})$ is the complementary error function defined as $1 - \mathrm{erf}(H\sqrt{t})$. The constant H is defined as

$$H = \frac{2\,\nu}{z_+^2\,\nu_+^2}\,\frac{\mathrm{R}\,T}{\mathrm{F}^2}\,\frac{1}{A\,\varepsilon\,c_0\,R_{\mathrm{LF},0}}\left[1+\frac{\partial \ln f_\pm(c_0)}{\partial \ln c}\right]\frac{(1-t_+(c_0))^2}{\sqrt{D^*_{\pm,\mathrm{eff}}(c_0)}} \quad [22]$$

According to Bard and Faulkner,[25] the factor $\exp(H^2 t)\mathrm{erfc}(H\sqrt{t})$ can be linearized for small values of $H\sqrt{t}$,

$$\exp\left(H^2\,t\right)\,\mathrm{erfc}\left(H\,t^{1/2}\right) \simeq 1 - \frac{2\,H}{\sqrt{\pi}}\sqrt{t} \quad [23]$$

In this case, Eq. 21 can be written as

$$I(t) = \frac{U_\mathrm{p}}{R_{\mathrm{LF},0}}\left(1-\frac{2\,H}{\sqrt{\pi}}\sqrt{t}\right) = I_0 - m_{\#3}\sqrt{t} \quad [24]$$

where $m_{\#3}$ denotes the slope of the current $I(t)$ with respect to $\sqrt{t}$. Thus at the beginning of a steady-state potentiostatic polarization, a linear relationship between the current flowing and the square root of time is expected.

Determination of the transference number based on the Sand equation, a concentration cell, and a known diffusion coefficient.— As already indicated in the literature survey, this method is the classical approach to determine the transference number of non-aqueous electrolytes. It is mainly used for polymer electrolytes as, e. g., in Ma et al.,[15] Ferry et al.[16] and Doeff et al.[17] In Zugmann et al., it is applied to a liquid electrolyte solution.[9] In contrast to the above described method, three experiments in two different experimental setups are necessary for the determination of the concentration dependent transference number $t_+(c)$. In a first step, the partial effective diffusion coefficient $D^*_{\pm,\mathrm{eff}}(c)$ ($\equiv \tau^{-1}\cdot D_\pm(c)$) is usually determined in a polarization cell as described, e.g., in Ehrl et al.[1] In a second step, the polarization cell can also be used for a second experiment, in which one can determine an additional factor of the form

$$f_1\left(f_\pm, t_+, {D^*_{\pm,\mathrm{eff}}}^{0.5}\right) \equiv \left[1+\frac{\partial \ln f_\pm(c_0)}{\partial \ln c}\right]\frac{(1-t_+(c_0))^2}{\sqrt{D^*_{\pm,\mathrm{eff}}(c_0)}} \quad [25]$$

However, to determine the transference number from the factor $f_1(f_\pm,\ t_+,\ {D^*_{\pm,\ \mathrm{eff}}}^{0.5})$ defined in Eq. 25 and the partial effective diffusion coefficient $D^*_{\pm,\ \mathrm{eff}}$, a third experiment is necessary. Thus, in order to close the system of equations, the factor $\left[1+\frac{\partial \ln f_\pm(c)}{\partial \ln c}\right](1-t_+(c))$ is determined in a concentration cell with transference[10] in a third step.

Sand equation (method #1).—The determination of the factor $f_1(f_\pm,\ t_+,\ {D^*_{\pm,\ \mathrm{eff}}}^{0.5})$ in Eq. 25 is based on the analysis of the short-term potential relaxation after a galvanostatic pulse polarization in a two-electrode cell. In this method, the Sand equation for the concentration difference Δc between anode and cathode at the current interruption time T_I (derived, e.g., in Bard and Faulkner, chapter 8.2.2[25]) is used to determine the factor $f_1(f_\pm,\ t_+,\ {D^*_{\pm,\ \mathrm{eff}}}^{0.5})$, i.e., the right-hand-side of Eq. 25 corresponds to

$$f_1\left(f_\pm,\ t_+,\ {D^*_{\pm,\ \mathrm{eff}}}^{0.5}\right)\Big|^{\text{pulse-polarization}}_{\text{short-term relax.}} = \frac{z_+^2\,\nu_+^2}{4\,\nu}\,\sqrt{\pi}\,\frac{\mathrm{F}^2}{\mathrm{R}\,T}\,A\,\varepsilon\,c_0\,\frac{U(T_\mathrm{I})}{I_\mathrm{p}\sqrt{T_\mathrm{I}}} \quad [26]$$

where the superscript of the function f_1 indicates that the excitation phase is a short-term pulse polarization (rather than a steady-state polarization) and the subscript indicates that the function is defined by the short-term behavior during the relaxation phase. Here, the correlation between concentration and potential introduced in the first part of this study is used.[1] $U(T_\mathrm{I})$ is the cell potential measured directly after current interruption. Therefore, the quality of the method can be improved further if the theoretical short-term relaxation behavior after the pulse is used to evaluate the cell potential $U(T_\mathrm{I})$ exactly at the current interruption time T_I. According to Hafezi and Newman,[26] the cell potential $U(t)$ is proportional to the artificial time τ^*

$$\tau^* = \frac{\sqrt{T_\mathrm{I}}}{\sqrt{t}+\sqrt{t-T_\mathrm{I}}} \quad [27]$$

For the determination of the transference number $t_+(c)$, the tortuosity τ of the porous medium is not required. The tortuosity τ of the porous medium is only necessary to get the binary diffusion coefficient $D_\pm(c)$ from the partial effective binary diffusion coefficient $D^*_{\pm,\mathrm{eff}}(c)$ measured by the methods introduced previously.[1]

Concentration cell.—In a concentration cell as introduced in the Experimental section, the measured cell potential equals the concentration overpotential. In the absence of kinetic reactions at the electrode for $I = 0$, the measured cell potential U is defined as

$$U = \int_\mathrm{C}^\mathrm{A}\nabla\Phi\,\mathrm{dx} = \frac{\nu}{z_+\nu_+}\,\frac{\mathrm{R}\,T}{\mathrm{F}}\int_\mathrm{C}^\mathrm{A}\left[\left[1+\frac{\partial \ln f_\pm(c_0)}{\partial \ln c}\right](1-t_+(c))\right]\cdot \mathrm{d}(\ln c) \quad [28]$$

The theoretical background for the derivation of Eq. 28 is discussed in the Theoretical background section in part I of this publication.[1] In accordance with the concentration profile in a polarization cell, A denotes the electrode which is in contact with the higher concentrated electrolyte solution and C the electrode which is in contact with lower concentrated electrolyte solution. The measured cell potential U is independent of the porosity ε and the tortuosity τ of the interconnecting separator. Based on experiments with various combinations of electrolytes with high and low salt concentrations, the factor $\left[1+\frac{\partial \ln f_\pm(c)}{\partial \ln c}\right](1-t_+(c))$ is fitted continuously by an n^{th} order polynomial.

Alternative methods for the determination of the transference number.— The factor $f_1(f_\pm,\ t_+,\ {D^*_{\pm,\ \mathrm{eff}}}^{0.5})$ cannot only be determined by the Sand equation, but also by alternative experiments in polarization cells. However, for some of these experiments, the factor $f_1(f_\pm,\ t_+,\ {D^*_{\pm,\ \mathrm{eff}}}^{0.5})$ is replaced by an alternative form

$$f_2\left(f_\pm, t_+, D^*_{\pm,\mathrm{eff}}\right) \equiv \left[1+\frac{\partial \ln f_\pm(c_0)}{\partial \ln c}\right]\frac{(1-t_+(c_0))^2}{D^*_{\pm,\mathrm{eff}}(c_0)} \quad [29]$$

Some methods from the literature as well as some novel approaches will be summarized and introduced in the following sections.

Long-term potentiostatic polarization (method #2).—The same framework as used for the direct determination of the transference number in Direct determination of the transference number by steady-state polarization experiments can also be embedded into a more general framework which is also valid for concentrated electrolyte solutions as discussed, e.g., in Doyle[22] and Ehrl.[23]

Based on Eqs. 1–6 and Eq. 16 as well as the basic differential equations and reformulations as given in the first part of this paper,[1] the factor $f_2(f_\pm,\ t_+,\ D^*_{\pm,\ \mathrm{eff}})$, i.e., the right-hand-side of Eq. 25 corresponds to

$$f_2\left(f_\pm,\ t_+,\ D^*_{\pm,\mathrm{eff}}\right)\Big|^{\text{ss polarization}}_{\text{transition period}} = \left[\frac{I_0\left(U_\mathrm{p}-\left(R_{\mathrm{LF,s}}-R_\mathrm{el}\right)I_\mathrm{s}\right)}{I_\mathrm{s}\left(U_\mathrm{p}-\left(R_{\mathrm{LF},0}-R_\mathrm{el}\right)I_0\right)}-1\right]\cdot\frac{\nu_+^2\,z_+^2}{\nu}\,\frac{\mathrm{F}^2}{\mathrm{R}\,T}\,\frac{A}{l}\,\varepsilon\,c_0\,R_\mathrm{el}. \quad [30]$$

where the superscript of the function f_2 indicates that the excitation phase is a steady-state polarization (rather than a pulse polarization) and the subscript indicates that the function is evaluated at the end of the polarization phase and at the beginning of the relaxation phase. An alternative formulation for Eq. 30 can be derived when the relation

for the initial low frequency resistance $R_{\mathrm{LF},0} = U_\mathrm{p}\,/I_0$ is used:

$$f_2\left(f_\pm,\ t_+,\ D^*_{\pm,\mathrm{eff}}\right)\Big|^{\text{ss polarization}}_{\text{transition period}} = \left[\frac{\left(U_\mathrm{p} - \left(R_{\mathrm{LF,s}} - R_\mathrm{el}\right) I_\mathrm{s}\right)}{I_\mathrm{s} R_\mathrm{el}} - 1\right]$$

$$\frac{\nu_+^2\, z_+^2}{\nu}\frac{\mathrm{F}^2}{\mathrm{R}\,T}\frac{A}{l}\varepsilon\, c_0\, R_\mathrm{el} = \left[\frac{U_\mathrm{p}}{I_\mathrm{s}} - R_{\mathrm{LF,s}}\right]\frac{\nu_+^2\, z_+^2}{\nu}\frac{\mathrm{F}^2}{\mathrm{R}\,T}\frac{A}{l}\varepsilon\, c_0 \qquad [31]$$

where the superscript of the function f_2 indicates that the excitation phase is a steady-state polarization and the subscript indicates that the function is defined by data from the very beginning of the polarization experiment and on the current/potential at the end of and after the steady-state polarization. As for the direct determination of the transference number, Eq. 31 is advantageous compared to Eq. 30, since less parameters have to be determined. Most important is this context is that the determination of the initial current flow I_0 which is required for Eq. 30 is challenging, as mentioned already before.

Initial time behavior of steady-state polarization (method #3).—The initial time behavior of the current following a steady-state polarization can also be used to determine the factor $f_1(f_\pm,\ t_+,\ D^{*\ 0.5}_{\pm,\ \mathrm{eff}})$ defined by Eq. 25. The basic derivation is given in Bard and Faulkner (chapter 5.5.1).[25] Based on the slope $m_{\#3}$ of the time dependent current given in Eq. 24, this factor, i.e., the right-hand-side of Eq. 25 corresponds to

$$f_1\left(f_\pm,\ t_+,\ D^{*\ 0.5}_{\pm,\ \mathrm{eff}}\right)\Big|^{\text{ss polarization}}_{\text{short-term pol.}} = \frac{z_+^2\ \nu_+^2}{4\ \nu}\sqrt{\pi}\frac{\mathrm{F}^2}{\mathrm{R}\ T} A\ \varepsilon\ c_0\ R_{\mathrm{LF},0}\frac{m_{\#3}}{I_0} \qquad [32]$$

where the superscript of the function f_1 indicates that the excitation phase is a steady-state polarization and the subscript indicates that the function is defined by the short-term behavior during the polarization phase. If the requirements for the linearization in Eq. 23 are not fulfilled, the additional information provided by Eq. 22 is limited, since the unknown factor H cannot be separated from the time t. The knowledge about the expected time behavior is also a good measure for the quality of experimental results.

Short-term relaxation from a steady-state concentration profile (method #4).—This method is based on the short-term relaxation behavior from a steady-state concentration profile as it has been used for the determination of the diffusion coefficient in the first part of this publication, starting with Eq. 16 in part I of this publication,[1] which can be reformulated to

$$U(t) = \underbrace{\frac{\nu}{Z_+^2\ \nu_+^2}\frac{\mathrm{R}\,T}{\mathrm{F}^2}\frac{l}{A\,\varepsilon\,c_0} I_\mathrm{s}\ f_2(f_\pm, t_+, D^*_{\pm,\mathrm{eff}})}_{U(T_\mathrm{I})} \cdot \left(1 - \underbrace{\sqrt{\frac{16\ D^*_{\pm,\mathrm{eff}}(c_0)}{\pi l^2}}\sqrt{t}}_{m_{\#4}}\right) \qquad [33]$$

by means of Eq. 8[1] with Eq. 9[1] and Eq. 5 of this paper. The basic mathematical methods are given in Bard and Faulkner (chapter A.1, A.1.4).[25] Eq. 33 describes the linear relaxation of the cell potential $U(t)$ with respect to $\sqrt{t}$ from its initial value $U(T_\mathrm{I})$ at the current interruption time T_I. Therefore, the factor $f_2(f_\pm,\ t_+,\ D^*_{\pm,\mathrm{eff}})$ described by the right-hand-side of Eq. 18 corresponds to

$$f_2\left(f_\pm,\ t_+,\ D^*_{\pm,\mathrm{eff}}\right)\Big|^{\text{ss polarization}}_{\text{short-term relax.}} = \frac{z_+^2 \nu_+^2}{\nu}\frac{\mathrm{F}^2}{\mathrm{R}T}\frac{A}{l}\varepsilon c_0\frac{U\,(T_\mathrm{I})}{I_\mathrm{s}} \qquad [34]$$

where the superscript of the function f_2 indicates that the excitation phase is a steady-state polarization and the subscript indicates that the function is defined by the short-term behavior during the relaxation phase. Here, the cell potential $U(T_\mathrm{I})$ is the potential measured directly after current interruption. The idea behind it is that the cell potential U immediately reduces to $U\ =\ \Delta\Phi$ upon switching to open circuit, whereas the concentration difference Δc will not have changed significantly, since diffusion takes place on a slower time scale. However, it is also difficult to determine the correct potential $U(T_\mathrm{I})$ directly after current interruption, since parasitic contributions interfere with the signal as a result of the concentration difference Δc between anode and cathode. To overcome this problem, the linear relation of the cell potential $U(t)$ with respect to $\sqrt{t}$ as derived in Eq. 33 can be used to determine the cell potential $U(T_\mathrm{I})$ exactly at the current interruption time T_I by means of extrapolation. In addition, the observation of the time behavior gives a good indication for the quality of experimental data.

Long-term relaxation from a steady-state profile (method #5).—As for the determination of the diffusion coefficient described in in part I of this publication,[1] the long-term relaxation behavior of the steady-state concentration profile at current interruption time T_I provides information for the determination of the factor $f_2(f_\pm,\ t_+,\ D^*_{\pm,\ \mathrm{eff}})$ defined by Eq. 18. In contrast to the determination of the diffusion coefficient, here a mathematical description for the prefactor C_1 is necessary (see Eq. 12 in Ref. 1). To be able to determine the prefactors C_{2n-1}, a steady-state concentration profile is required as initial condition, whereas it is arbitrary how the steady-state concentration profile is obtained. The derivation is discussed, e.g., in Polifke and Kopitz[27] (chapter 14.1) or in Ehrl.[23] As a result, the time dependent concentration difference $\Delta c(t)$ can be expressed as

$$\Delta c\,(t)\ =\ 8\frac{\Delta \mathrm{c}\,(T_\mathrm{I})}{\pi^2}\exp\left(-\frac{\pi^2 D^*_{\pm,\mathrm{eff}}\,(c_0)}{l^2}t\right) \qquad [35]$$

Higher order terms are already neglected in Eq. 35. As usual, the expression for the concentration difference $\Delta c(t)$ given in Eq. 35 can be related to the potential U as explained in the section Theoretical background of the first part of this study:[1]

$$\ln U\,(t) = \ln\left(\frac{8\ \nu}{z_+^2\ \nu_+^2}\frac{\mathrm{R}\ T}{\mathrm{F}}\left[1 + \frac{\partial \ln f_\pm\,(c_0)}{\partial \ln c}\right](1 - t_+\,(c_0))\frac{1}{\pi^2}\frac{\Delta c\,(T_\mathrm{I})}{c_0}\right) - \frac{\pi^2 D^*_{\pm,\mathrm{eff}}\,(c_0)}{l^2}t\ =\ O\,(T_\mathrm{I})\ -\ \frac{\pi^2 D^*_{\pm,\mathrm{eff}}\,(c_0)}{l^2}t \qquad [36]$$

The long-term relaxation of the cell potential $\ln U(t)$ is proportional to the time t, whereas $O(T_\mathrm{I})$ stands for the first term on the right hand side of the equation, which corresponds to the value of $\ln U(t)$ extrapolated to time T_1 in the relaxation phase (shown later in the lower inset of Figure 3b). Based on the constant factor $O(T_\mathrm{I})$ and Eq. 5, it is possible to find the following relationship for the right-hand-side of the factor $f_2(f_\pm,\ t_+,\ D^{*\ }_{\pm,\ \mathrm{eff}})$ defined in Eq. 29

$$f_2\left(f_\pm,\ t_+,\ D^*_{\pm,\mathrm{eff}}\right)\Big|^{\text{ss polarization}}_{\text{long-term relax.}} = \frac{z_+^2\ \nu_+^2}{8\ \nu}\ \pi^2\frac{\mathrm{F}^2}{\mathrm{R}\ T}\frac{A}{l}\varepsilon\ c_0\frac{\exp\ O\ (T_\mathrm{I})}{I_\mathrm{s}} \qquad [37]$$

where the superscript of the function f_2 indicates that the excitation phase is a steady-state polarization and the subscript indicates that the function is defined by the long-term behavior during the relaxation phase.

Transference number based on data from a concentration cell and a ferrocene cell.—The transference number can also be determined by only two different types of experiments using a concentration cell and our previously described method for determining the thermodynamic factor $\left(\mathrm{TDF} \equiv \left[1 + \frac{\partial \ln f_\pm(\mathrm{c})}{\partial \ln c}\right]\right)$,[2] which is based on measuring the lithium concentration dependent potential of a lithium electrode versus ferrocene/ferrocenium as introduced in Landesfeind et al.[2] (further on referred to as ferrocene cell measurements). Based on a functional description of the TDF and the experimental data obtained by a concentration cell with transference[10] (see the above Concentration cell section), it is possible to solve for the

concentration dependent transference number from the relation given in Eq 28.

No restrictions regarding the concentration dependence of the transport parameters have been introduced so far. For a known functional description of the concentration dependent transference number $t_+(c)$ and for many experiments with different combinations of c_A and c_C covering the concentration range of interest, it is possible to determine the necessary functional parameters of the predefined function by numerical fitting. However, the functional description of the concentration dependent transference number $t_+(c)$ is usually not known a priori.

An alternative approach is to assume a constant transference number within a narrow concentration range centered about an average concentration of c_0, expressed as $c_0 \pm \delta c$ (with $\delta c \ll c_0$), so that one can determine an average transference number within a differential concentration range, i.e., $t_+(c_0 \pm \delta c)$. In this case, Eq. 28 can be approximated by

$$t_+(c_0 \pm \delta c) \approx 1 - \frac{z_+ \nu_+}{\nu} \frac{\mathrm{F}}{\mathrm{R}\,T} U \left[\int_{c_0-\delta c}^{c_0+\delta c} \left[1 + \frac{\partial \ln f_\pm(c)}{\partial \ln c} \right] \mathrm{d}(\ln c) \right]^{-1}$$

$$\approx 1 - \frac{z_+ \nu_+}{\nu} \frac{\mathrm{F}}{\mathrm{R}\,T} U \left[\int_{c_0-\delta c}^{c_0+\delta c} \mathrm{TDF}(c)\, \mathrm{d}(\ln c) \right]^{-1} \quad [38]$$

where TDF(c) represents the concentration dependent thermodynamic factor. Compared to all other methods introduced for the determination of the concentration dependent transference number $t_+(c)$, this last described approach requires no assumptions other than that the transference number can be assumed constant within a differential concentration range (i.e., that it be a smooth function with concentration). In the following this method is called the δc method.

Numerical Validation

In the following, the analytical expressions for the determination of the transference number t_+ introduced in the Theory section are analyzed in terms of their potential applicability for the experimental determination of the transference number by means of numerical simulations. Simulations are performed with a finite element research code developed at the Institute for Computational Mechanics at the Technical University of Munich. A detailed derivation to the used numerical methods is given in Ehrl.[23] The used governing equations as well as the corresponding boundary condition are given in the first part of this publication (Eq. 1 to 3 and Eq. 5) together with setup, boundary conditions, and parameters used for the simulation.[1]

Numerical analysis of the polarization experiments.—In the following, the transference number t_+ is calculated from the factors $f_1(f_\pm,\ t_+,\ D^*_{\pm,\mathrm{eff}})$ or $f_2(f_\pm,\ t_+, D^{*\ 0.5}_{\pm,\ \mathrm{eff}})$ defined in Eq. 25 and 29, respectively, the value of which be determined by the five different methods introduced in the Theory section and summarized in Table I. In contrast to the experimental approach introduced in the section Transference number based on data from a concentration cell and a ferrocene cell, in this section the transference number is not calculated based on data from a concentration cell but based on a given thermodynamic factor TDF(c). Our newly proposed method for the direct determination of the transference number will be discussed later on.

As shown in Figure 2, a pulse polarization experiment consists of a polarization and relaxation phase. During the short-term polarization phase, a short galvanostatic pulse with the current I_p is applied until the current interruption time T_I to establish a concentration gradient within the two-electrode cell. The concentration difference $\Delta c(t)$ between anode and cathode develops according to the Sand equation given in, e.g., Bard and Faulkner.[25] During this phase, the cell potential $U(t)$is influenced by the concentration difference $\Delta c(t)$, the current flow I_p, and kinetic effects at the electrode. At the time $t = T_\mathrm{I}$, the current I_p is interrupted. During the following relaxation phase, the concentration difference $\Delta c(t)$ as well as the corresponding cell potential $U(t)$ slowly relax with time. In contrast to the polarization phase, the cell potential $U(t)$ is only influenced by the concentration difference $\Delta c(t)$. As long as the applied polarization current I_p is small, a linear relationship between the cell potential $U(t)$ and the concentration difference $\Delta c(t)$ can be assumed, as explained in the Theoretical background section in the first part of this publication.[1] In this case, the non-linearities introduced by the concentration dependence of the transport parameters and by the linearization of the natural logarithm are negligibly small.

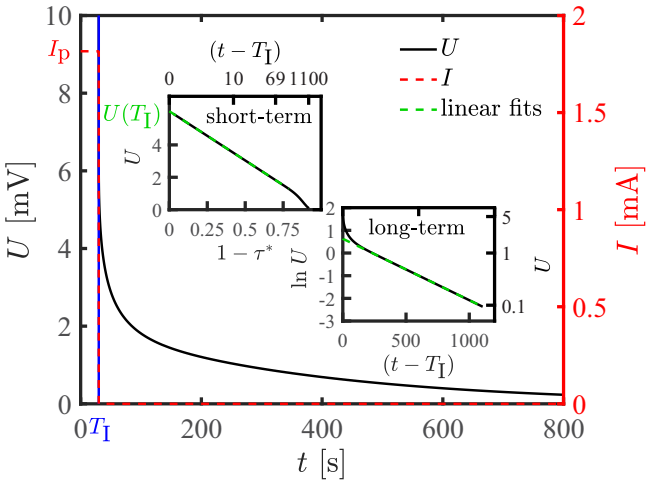

Figure 2. Simulation of a short-term galvanostatic pulse experiment according to the parameters given in Table I in Ref. 1 with a polarization time of 30 s, a polarization current density $i_\mathrm{p} = 8 \cdot 10^{-3}$ mA mm^{-2} corresponding to the polarization current $I_\mathrm{p} = 1.82$ mA and an initial electrolyte concentration $c_0 = 1$ M.

The expected linear behavior of the cell potential $U(t)$ with respect to the artificial time τ^* for the short-term relaxation as well as the linear behavior of the cell potential $\ln U(t)$ with respect to the time $(t - T_\mathrm{I})$ for the long-term relaxation are clearly observable for reasonable time periods in Figure 2. Since the determination of the factor $f_1(f_\pm,\ t_+,\ D^{*\ 0.5}_{\pm,\ \mathrm{eff}})|^{\text{pulse polarization}}_{\text{short-term relax.}}$ according to Eq. 26 (method #1) is based on the cell potential $U(T_\mathrm{I})$ at the current interruption time, the linearity in τ^* can be used to more accurately determine the cell potential $U(T_\mathrm{I})$ at current interruption time T_I. This is particularly important for experiments where the cell potential $U(t)$ is influenced by additional parasitic contributions as, e.g., the discharge of the double layer. While not evident from the upper inset in Figure 2 by eye, the simulated transient approaches the real axis for long times, i.e., $1 - \tau^* \to 1$, which is automatically fulfilled as the potential relaxes to 0 mV for long real times.

A steady-state polarization experiment also consists of two phases. In the first phase shown in Figure 3a, the two-electrode cell is polarized with a constant cell potential U_p (black line) until the steady-state current I_s is established (red dashed line). The steady-state current I_s is reached once a steady-state concentration profile within the cell is established. The electrode kinetics are modeled by a Butler-Volmer law without concentration dependence (i.e., $\gamma = 0$), resulting in a constant interface resistance R_I due to the linearity of the Butler-Volmer law for small surface overpotentials η. The initial current I_0 is the maximum current value obtained during polarization, since the concentration overpotential is negligibly small in the beginning. Due to an increasing concentration overpotential with time, the current $I(t)$ decreases with time until the steady-current I_s is reached. For concentrated electrolyte solutions, a steady-state experiment can be used to determine the factor $f_2(f_\pm,\ t_+,\ D^*_{\pm,\mathrm{eff}})|^{\text{ss polarization}}_{\text{transition period}}$ by method #2. The short-term relaxation of the current $I(t)$ is linear with respect to $\sqrt{t}$, with the slope $m_{\#3}$ (see inset of Figure 3a). As shown in the section Initial time behavior of steady-state polarization *(*method #3*)*, this is already an approximation for the more complex function $\exp(H^2\, t)\mathrm{erfc}(H\, \sqrt{t})$ given in Eq. 23. Based on the here obtained

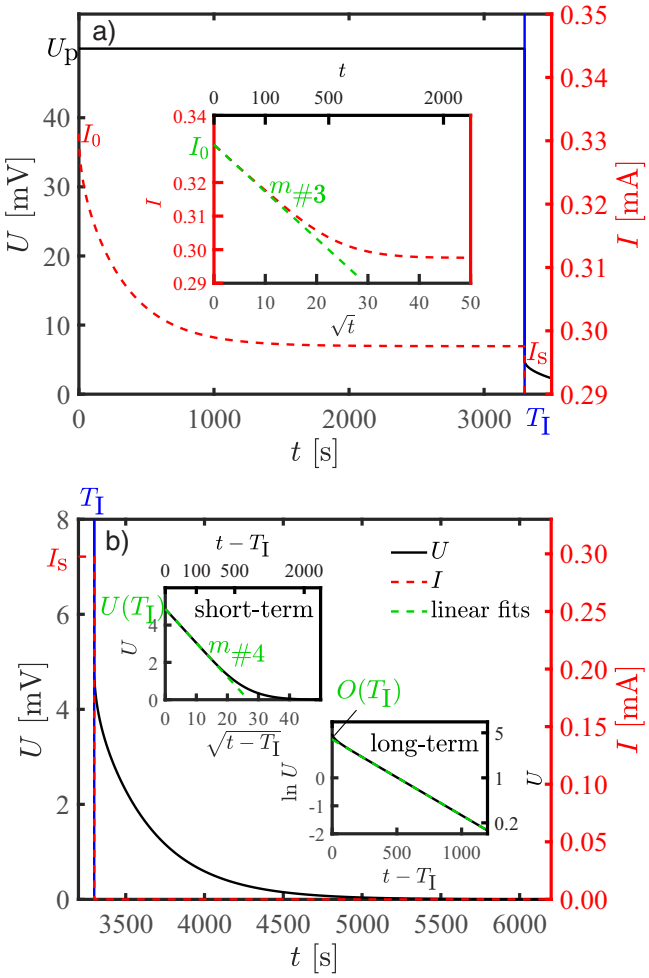

Figure 3. Simulation of a steady-state polarization experiment according to the parameters given in Table II in Ref. 1, with a polarization time $T_I = 3300$ s, a polarization potential $U_p = 50$ mV, and an initial electrolyte concentration $c_0 = 1$ M: a) polarization phase showing potential (black line) and current (red dashed line) vs. time as well as current vs. $\sqrt{t}$; b) relaxation phase showing potential (black line) and current (red line) vs. time, with the insets showing the short-term and long-term relaxation of the potential.

slope $m_{\#3}$, the factor $f_1(f_\pm, t_+, D^{*}_{\pm,\,\mathrm{eff}}{}^{0.5})|^{\text{ss polarization}}_{\text{short-term pol.}}$ can be calculated by Eq. 32.

Once the steady-state current I_s is reached, the polarization of the cell is interrupted and the relaxation phase of the steady-state experiment starts. During the relaxation phase, the cell potential $U(t)$ decreases continuously as shown in Figure 3b. The time for the relaxation process is much longer than in a pulse experiment because of the larger changes to the salt concentration profile. The long-term behavior of the relaxation process is characterized by a linear relationship between $\ln U$ and $(t - T_I)$ (see lower inset in Figure 3b), from which the value of $O(T_I)$ can be obtained by extrapolation to $(t - T_I) = 0$; from the latter, the factor $f_2(f_\pm, t_+, D^{*}_{\pm,\mathrm{eff}})|^{\text{ss polarization}}_{\text{long-term relax.}}$ can be calculated according to Eq. 37 (method #5). Different from a pulse experiment, the short-term relaxation behavior of the cell potential $U(t)$ in a steady-state experiment is proportional to $\sqrt{t}$, with the slope m_{sqrt} (see upper inset in Figure 3b). The extrapolated cell potential $U(T_I)$ at current interruption time T_I can be used to calculate the factor $f_2(f_\pm, t_+, D^{*}_{\pm,\mathrm{eff}})|^{\text{ss polarization}}_{\text{short-term relax}}$ with Eq. 34 (method #4).

Validation of the different parameter determination methods.— In the following, we numerically analyze how well the assumptions made in the theoretical part of this work are met when trying to determine the various transport parameters from simulated transients. For example, the influence of non-negligible concentration variations between anode and cathode and their impact on the determined diffusion coefficients and transference numbers will be evaluated in the following.

Influence of the magnitude of the concentration difference.—In Figure 4, the influence of the concentration difference $\Delta c(T_I) = c_A(T_I) - c_c(T_I)$ between the two electrodes at current interruption time T_I is investigated numerically for a bulk salt concentration of $c_0 = 1$ M. In the case of a steady-state experiment, the concentration difference $\Delta c(T_I)$ defined by the polarization cell potential U_p is the only design parameter influencing the quality of the determined transference number.

All methods summarized in Table I are capable to determine the correct transference number t_+ for a small concentration difference $\Delta c(T_I)$. For higher concentration differences $\Delta c(T_I)$, it is not possible to determine the transference accurately by the short-term transient of a steady-state polarization experiment (method #3; red diamond in Figure 4), which is based on the initial time behavior of the current $I(t)$ during the polarization phase in a steady-state experiment. In this case, the initial time behavior is not just influenced by concentration dependent transport parameters and the linearization of the natural logarithm introduced in Eq. 9 in part I of this publication (Ref. 1), but also by the basic characteristic of the electrode kinetics. For an increasing concentration difference $\Delta c(T_I)$ and therefore an increasing current flow, the Butler-Volmer law cannot be assumed linear anymore, which violates the linear boundary condition used for the derivation of Eq. 32. As a result, the linear behavior of the current $I(t)$ can only be observed clearly for the lowest polarization potential U_p (i.e., for the lowest concentration difference). For this method, the linearity of the current vs. $\sqrt{t}$ (see inset of Figure 3a) is a very good indication for the reliability of experimentally measured data, and therefore the method is only considered in the Results and discussion section, if a clear linear trend is observable. All remaining methods are accurate up to relative concentration differences $\Delta c(T_I)/c_0$ of about

Table I. Overview of the five analytical methods described in the text for the determination of the transference number from polarization cell experiments. Here, the right-hand-side of the definitions of the factors $f_1(f_\pm, t_+, D^{*}_{\pm,\,\mathrm{eff}}{}^{0.5})$ (Eq. 25) and $f_2(f_\pm, t_+, D^{*}_{\pm,\,\mathrm{eff}})$ (Eq. 29) equate to the terms shown in this table. The superscripts in the functions f_1 and f_2 refer the excitation phase (either pulse or steady-state polarization) and the subscripts refers to where the function is being evaluated (from the short- or long-term behavior during either the excitation or the subsequent relaxation phase).

method #1	$f_1(f_\pm, t_+, D^{*}_{\pm,\,\mathrm{eff}}{}^{0.5})\|^{\text{pulse polarization}}_{\text{short-term relax.}}$	$\frac{z_+^2\,\nu_+^2}{4\,\nu}\sqrt{\pi}\frac{\mathrm{F}^2}{\mathrm{R}\,T}\,A\,\varepsilon\,c_0\frac{U(T_I)}{I_p\sqrt{T_I}}$	Eq. 26
method #2	$f_2(f_\pm, t_+, D^{*}_{\pm,\mathrm{eff}})\|^{\text{ss polarization}}_{\text{transition period}}$	$\left[\frac{U_p}{I_s} - R_{\mathrm{LF,s}}\right]\frac{\nu_+^2\,z_+^2}{\nu}\frac{\mathrm{F}^2}{\mathrm{R}\,T}\frac{A}{l}\varepsilon\,c_0$	Eq. 31
method #3	$f_1(f_\pm, t_+, D^{*}_{\pm,\,\mathrm{eff}}{}^{0.5})\|^{\text{ss polarization}}_{\text{short-term pol.}}$	$\frac{z_+^2\,\nu_+^2}{4\,\nu}\sqrt{\pi}\frac{\mathrm{F}^2}{\mathrm{R}\,T}\,A\,\varepsilon\,c_0\,R_{\mathrm{LF},0}\frac{m_{\#3}}{I_0}$	Eq. 32
method #4	$f_2(f_\pm, t_+, D^{*}_{\pm,\mathrm{eff}})\|^{\text{ss polarization}}_{\text{short-term relax.}}$	$\frac{z_+^2\,\nu_+^2}{\nu}\frac{\mathrm{F}^2}{\mathrm{R}\,T}\frac{A}{l}\varepsilon\,c_0\frac{U(T_I)}{I_s}$	Eq. 34
method #5	$f_2(f_\pm, t_+, D^{*}_{\pm,\mathrm{eff}})\|^{\text{ss polarization}}_{\text{long-term relax.}}$	$\frac{z_+^2\,\nu_+^2}{8\,\nu}\pi^2\frac{\mathrm{F}^2}{\mathrm{R}\,T}\frac{A}{l}\varepsilon\,c_0\frac{\exp\,O(T_I)}{I_s}$	Eq. 37

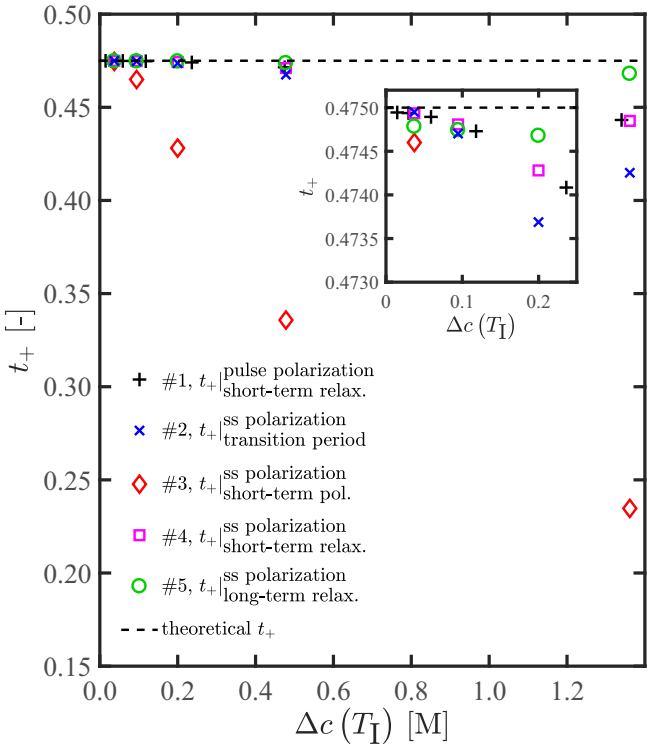

Figure 4. Influence of the concentration difference $\Delta c(T_\mathrm{I})$ at the current interruption time on the determined transference number for a $c_0 = 1$ M electrolyte solution (see Table II in Ref. 1 for other simulation parameters).

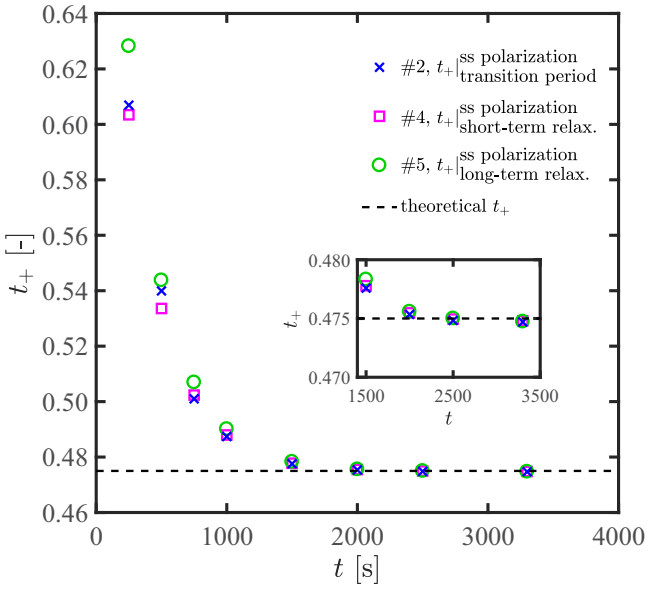

Figure 5. Influence of the polarization time in nominally steady-state polarization experiments on the determined transference number t_+ for a polarization potential $U_\mathrm{p} = 50$ mV and an initial concentration $c_0 = 1$ M (see Table II in Ref. 1 for simulation parameters).

20%. Particularly the method $f_2(f_\pm,\ t_+,\ D^*_{\pm,\mathrm{eff}})|^{\text{ss polarization}}_{\text{long-term relax.}}$ (green circles in Figure 4) is very accurate for higher polarization potentials, since it is based on the long-term relaxation behavior, where the requirement of a small concentration difference between the electrodes is automatically fulfilled at long times. Similar results are obtained for a bulk salt concentration of $c_0 = 0.01$ M and $c_0 = 2.0$ M which are not shown explicitly in this publication.

As explained under Direct determination of the transference number by steady-state polarization experiments, the transference number t_+ can also be calculated directly from Eq. 18 for dilute electrolyte solutions. The method is based on the steady-state current I_s, the steady-state low frequency resistance R_LF, the electrolyte resistance R_el and the polarization potential U_p. For the smallest polarization potential U_p, the calculated transference numbers t_+ are 0.32, 0.525 and 0.465 for the concentrations 0.01 M, 1 M and 2 M, respectively. For these concentrations the transference numbers resulting from the defined simulation parameter given in Table II in part I of this publication (Ref. 1) are 0.402, 0.475 and 0.3. Even for smaller concentrations c_0, the expected transference number t_+ cannot be determined correctly, since the mathematical condition given in Eq. 17 is not fulfilled for the used parameter set and for $c_0 \to 0$. Theoretically, Eq. 17 could be used as an additional condition for the determination of the parameter set for very dilute electrolyte solutions (i.e., as $c_0 \to 0$), but the experimental methods discussed in the first and the second part of this paper are not designed to determine the transport parameters at very dilute solutions, as will be explained in Results and discussion.

Influence of a non steady-state concentration profile on the determination of the transference number.—Although the concentration difference $\Delta c(T_\mathrm{I})$ at the current interruption time is the only design parameter in a steady-state experiment which can be influenced by experimental design, it is possible that a non-steady-state concentration profile at the current interruption time for an intended steady-state polarization experiments leads to an incorrect determination of the transference number. A non-steady-state concentration profile originates from too short polarization times or from the continuous variation of the interface resistance R_I during a steady-state experiment. The influence of a non-steady-state concentration profile as a result of too short polarization times on the determined transference number is depicted in Figure 5 for all corresponding methods. The method $t_+|^{\text{ss polarization}}_{\text{short-term pol.}}$ (#method 3) is not considered here since it does not rely on a steady-state concentration profile but only on the short-term behavior of the steady-state polarization experiment. The presented numerical data are the results for a bulk salt concentration of $c_0 = 1$ M polarized with a cell potential of $U_\mathrm{p} = 50$ mV. This applied cell potential results in concentration difference $\Delta c(T_\mathrm{I})$ at current interruption (steady-state) of 0.1 M, which corresponds to $\frac{\Delta c(T_\mathrm{I})}{c_0} = 10\%$. The error for the transference number t_+ based on a polarization time between 1000 and 1500 s is still below 5% (see Figure 5). For polarization times $t > 1500$ s, the correct transference number is obtained for all analysis methods. For short polarization times $t < 1000$ s, the error in the transference number t_+ increases rapidly (see Figure 5), because of the large deviation from the steady-state concentration profile.

The relaxation of the current $I(t)$ during the polarization is shown in Figure 6a, while Figure 6b shows the relaxation behavior of the relative cell potential $U(t)/U(T_\mathrm{I})$ with respect to $\sqrt{t}$ for differently chosen polarization times (indicated by the dashed vertical lines in Figure 6a). Only after a polarization time of $t \approx 1000 - 1500$ s, the current $I(t)$ approaches its steady-state value as shown in Figure 6a and the relative cell potential $U(t)/U(T_\mathrm{I})$ exhibits a clear linear behavior with respect to $\sqrt{t}$, as depicted in Figure 6b. While for shorter polarization times, the current is obviously still quite different from its steady-state value (see Figure 6a), the corresponding non-linearity of the relative cell potential $U(t)/U(T_\mathrm{I})$ during subsequent relaxation is unfortunately not very apparent, as is illustrated by the $U(t)/U(T_1)$ response for a polarization time of $T_1 = 500$ s (see blue dash-dotted line in Figure 6b). For longer polarization times of $T_1 = 1000$ s, $T_1 = 1500$ s, and $T_1 = 3000$ s, the shape of the scaled relaxation curve $U(t)/U(T_1)$ cannot be differentiated from Figure 6b (corresponding magenta, red and black lines overlap). Therefore, it is important for a steady-state experiment to carefully observe the relaxation behavior of the current $I(t)$ during polarization as well as the relaxation behavior of the cell potential $U(t)$ after current interruption in order to ensure a steady-state concentration profile. Numerical simulations indicate that a similar behavior can be expected for a concentration profile

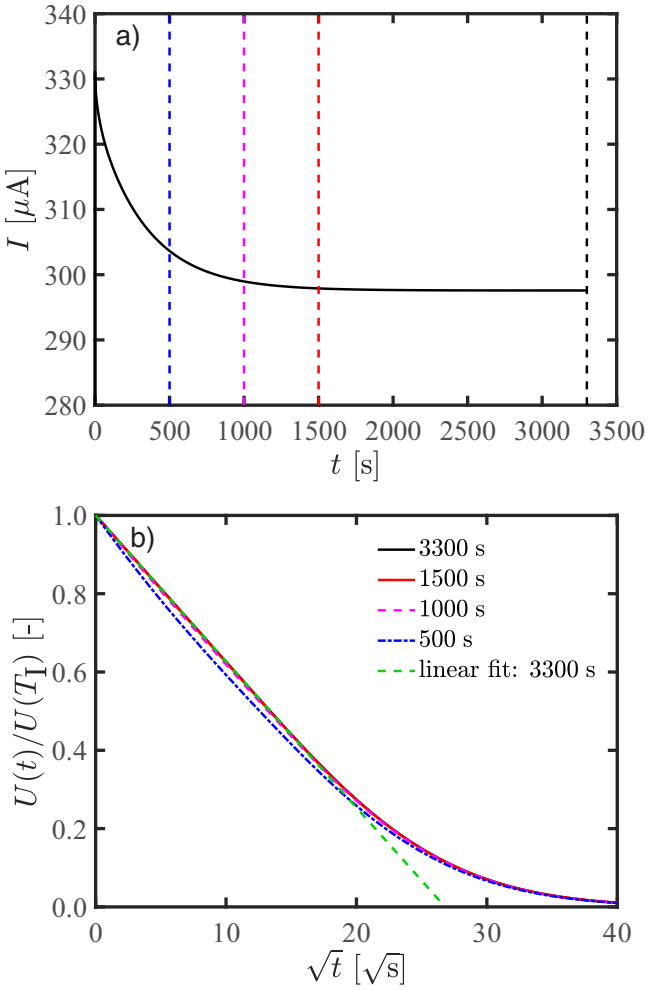

Figure 6. Polarization and relaxation phase of a nominally steady-state polarization experiment according to the simulation parameters given in Table II of Ref. 1 with the polarization potential $U_p = 50$ mV and the intial concentration $c_0 = 1$ M: a) current I over time t during the initial polarization phase; b) relative cell potential $U(t)/U(T_I)$ vs. $\sqrt{t}$ during the relaxation phase following the initial polarization after different current interruption times T_I, indicated by the dashed vertical lines in a). Transients for T_I= 3300 s, 1500 s, and 500 s in b) overlap in the entire time range shown and are not distinguishable by eye.

deviating from its steady-state value as a result of a continuously varying interface resistance R_I.

Influence of the polarization time on the determined transference number in a pulse experiment.—For the determination of the transference number $t_+|^{\text{pulse polarization}}_{\text{short-term relax.}}$ (#method 1), a galvanostatic pulse experiment has to be performed as indicated in Figure 2. In this experimental setup, the concentration difference $\Delta c(T_I)$ is influenced by the polarization current I_p and the polarization time defined by the current interruption time T_I.[25] As shown discussed in the section Influence of the magnitude of the concentration difference, both design parameters have to be chosen so that the relative concentration difference $\Delta c(T_I)/c_0$ does not exceed 20%. Additionally, the current interruption time T_I has to be short enough to ensure that the semi-infinite boundary condition used for the derivation of Eq. 26 is not violated. For longer polarization times, the concentration profile will slowly approach the steady-state case, which must not happen for a pulse experiment. In Figure 7, the calculated transference number t_+ with respect to the polarization time for a 1 M electrolyte solution polarized with a current density of $I_p = 0.454$ mA is depicted.

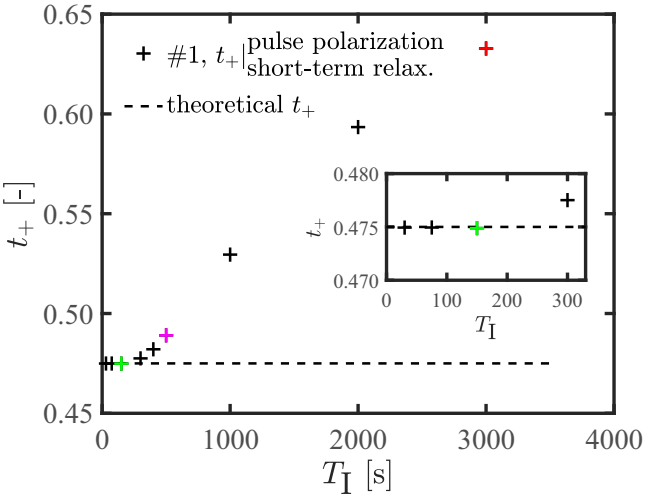

Figure 7. Influence of the polarization time in a pulse experiment on the determined transference number t_+ for a polarization current of $I_p = 0.454$ mA and an initial concentration $c_0 = 1$ M (see Table II in Ref. 1 for simulation parameters). The colored crosses at times 150 s, 500 s, and 3000 s correspond to the coloring of the transients plotted in Figure 8.

As can be seen in Figure 7, for polarization times of about 500 s, the deviation of the determined transference number is below 5%. The corresponding relaxation behavior of the relative cell potential $U(t)/U(T_I)$ with respect to the artificial time $1 - \tau^*$ and the time $\sqrt{(t - T_I)}$ are shown in Figure 8a and Figure 8b, respectively. Figure 8b is added, since for longer polarization time the concentration profile approaches steady-state which results in a linear relaxation behavior of the cell potential with respect to time $\sqrt{(t - T_I)}$. Additionally, simulations with shorter and longer polarization times are shown to visualize the differences.

Figure 8a depicts the short-term relaxation of the potential after a pulse polarization which can be used for evaluation of the transference number according to method #1 (see Eq. 26). This method is valid for short polarization times, i.e., a steady-state concentration profile is not reached yet but only the electrolyte concentration at the vicinity of the electrodes is changed, which is the case for the 150 s polarization (green line in Figure 8). For this short polarization time, the linear behavior in Figure 8a is prominent and the typical S-shape can be observed (compare inset in Figure 2). This shape, i.e., an initial linear slope (green line between 0 and 0.5), followed by a steeper decline (green line between 0.7 and 0.8) eventually approaching the x-axis (green line beyond 0.8), cannot be observed for the longest polarization time of 3000 s. Note that the S-shape in Figure 8a and in Figure 2 is only partly visible as this would require much longer simulation times, the slow approach to the real axis will be automatically fulfilled as $U \to 0$ mV for $t \to \infty$. Although for all polarization times an initially linear behavior can be observed, the steeper section of the potential relaxation is missing for long pulse durations (compare Figure 8a for pulse duration of 3000 s, red line), making this part a distinguishable feature for whether or not the transference number can be determined by using method #1. Figure 8b also shows the short-term behavior of the potential relaxation, i.e., the same data as in Figure 8a but plotted on a different scale. Comparison of Figure 8b with the inset of Figure 3b shows that a steady state concentration profile is reached for the polarization time of 3000 s, evident through the linear potential relaxation with $\sqrt{(t - T_I)}$ (compare black dashed linear trend in Figure 8b). From Figure 8 it is concluded that method #1 yields the most accurate results for the transference number when the potential relaxation after a pulse polarization with $1 - \tau^*$ shows the typical S-shape and when the same relaxation data do not show a pronounced linear behavior with $\sqrt{(t - T_I)}$ which can be seen exemplarily for the shortest polarization time of 150 s in Figure 8. While

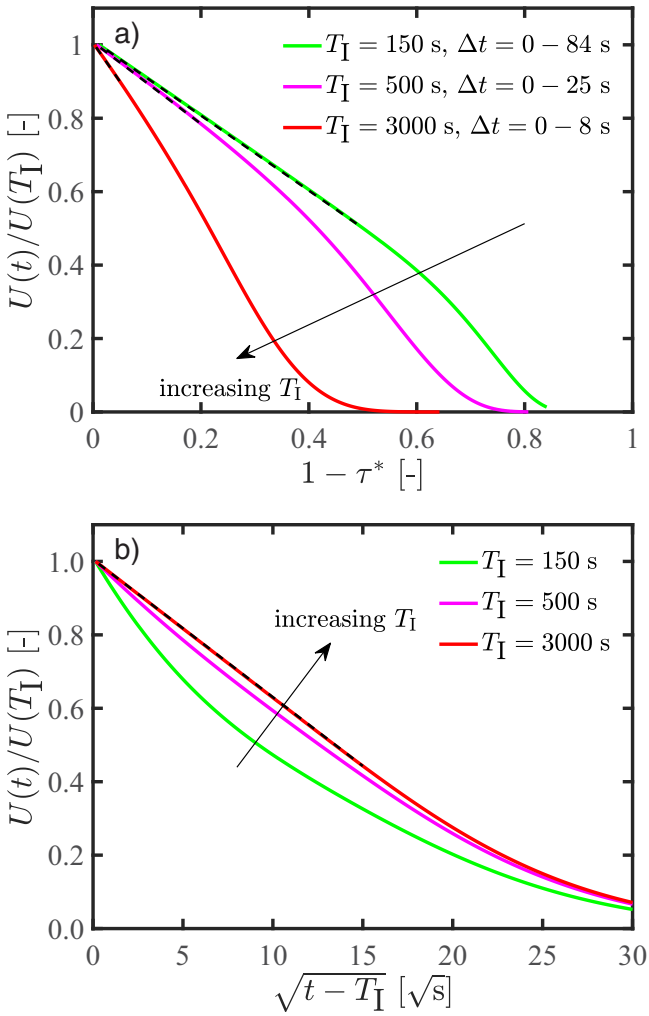

Figure 8. Relaxation behavior of the relative cell potential $U(t)/U(T_I)$ after pulse experiment with a polarization current of $I_p = 0.454$ mA and an initial concentration $c_0 = 1$ M (see Table II in Ref. 1 for simulation parameters): a) the artificial time $1 - \tau^*$ and b) the time $\sqrt{(t - T_I)}$. Black dashed lines indicate the linear ranges that would be used for analysis of experimental data. In a) the real times are given in the respective legends, in b) only the linear trend for $T_I = 3000$ s can be used for analysis.

in the computer simulations shorter polarization times yield smaller errors (compare Figure 7), in an experiment the experimental noise of, e.g., the potential measurement has to be considered and the pulse duration cannot be too short as the resulting concentration change would be too small to be measurable without large uncertainty.

Results and Discussion

In this section, we will present our new proposed method to determine the transference number from two sets of experiments: concentration cell measurements with a series of small concentration differences combined with the concentration dependent thermodynamic factor (TDF) obtained with a cell in which the potential of a lithium electrode vs. a ferrocene/ferrocenium reference electrode is measured for different lithium salt concentrations (referred to as "ferrocene cell").[2] The concentration dependence of the transference number obtained by this method will subsequently be compared with the values obtained by the various polarization methods (see Table I) in combination with a concentration cell.

Transference number based on data from a concentration cell and a ferrocene cell.—In the following, the transference number

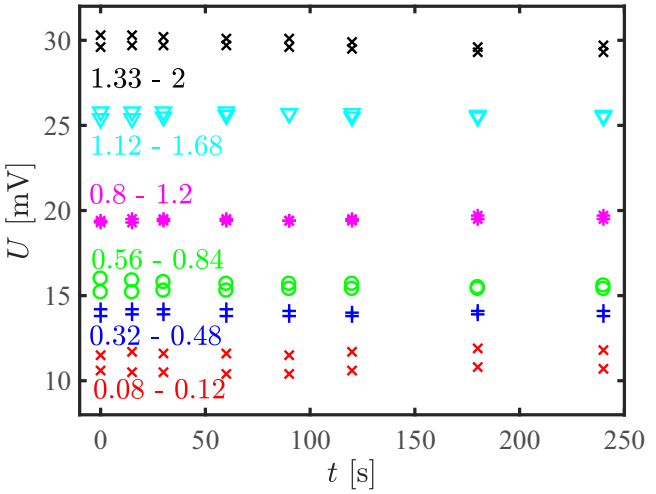

Figure 9. Exemplary concentration cell potentials for the δc method versus time for EC:DEC (1:1 w:w) based electrolytes, measured for differential $LiClO_4$ concentrations as given in the figure. Measurement were conducted in a temperature controlled glove box with the cell setup depicted in Figure 1. Two individual sets of measurements for each pair of concentrations (see legend in the figure) are depicted to illustrate the reproducibility of the measurements.

of the lithium ion will be determined from measurements with a concentration cell (see Figure 1) in combination with the concentration dependent thermodynamic factor obtained by ferrocene cell measurements for the same electrolyte taken from Figure 9 in the study by Landesfeind et al.[2] Exemplary concentration cell potentials (corresponding to concentration overpotentials) depicted in Figure 9 show the stability of the potential measurements over time and their reproducibility.

The measured concentration overpotentials are linearly extrapolated to t = 0 s and the obtained initial potentials were averaged. The variation between repeat measurements is <1.5 mV at the beginning of the measurement and differs by <1.5 mV over the course of the measurement period. As the standard deviations of latter averages are generally smaller than the accuracy of the potential measurement of 0.3 mV, only the error from the measurement device is considered in the following. Figure 9 shows exemplary measurements of our here proposed δc method, for which the concentration overpotentials between two electrolytes of similar concentrations centered about an average concentration $c_0 \pm \delta c$ are measured, whereby δc is a sufficiently small such that the transference number can be assumed constant. The advantage of this approach is that no functional for the transference number has to be assumed and that a pointwise calculation is possible to yield the average transference number $t_+(c_0 \pm \delta c)$ within a sufficiently small δc range as shown by Eq. 38. Analogously to Figure 9, also concentration cells with larger concentration differences were measured, with the results being displayed in Figure 11. As the concentration overpotential for larger concentration differences increases, the relative error gets smaller and exemplary data are thus not shown.

In combination with Eq. 38 and with the concentration dependent thermodynamic factor for this electrolyte (see Figure 9 in Reference 2), the values of $t_+(c_0 \pm \delta c)$ vs. concentration depicted in Figure 10 can be obtained, whereby the used values of δc are represented by the x-error bars. Additionally, Figure 10 shows a quadratic fit based on data from the δc method, with its 95% confidence interval as gray highlighted area. The obtained functional description is given by

$$t_+ \ (c \pm \delta c) = -0.117\, c^2 + 0.171\, c + 0.472 \qquad [39]$$

The transference number shows a peak around a concentration of 0.8 M $LiClO_4$, with a value of $t_+ \approx 0.53$. For $c \to 0$, we find a value of $t_+ \approx 0.47$, while at 2 M $LiClO_4$ concentration the transference number drops to $t_+ \approx 0.35$. For the following analysis, the transference number

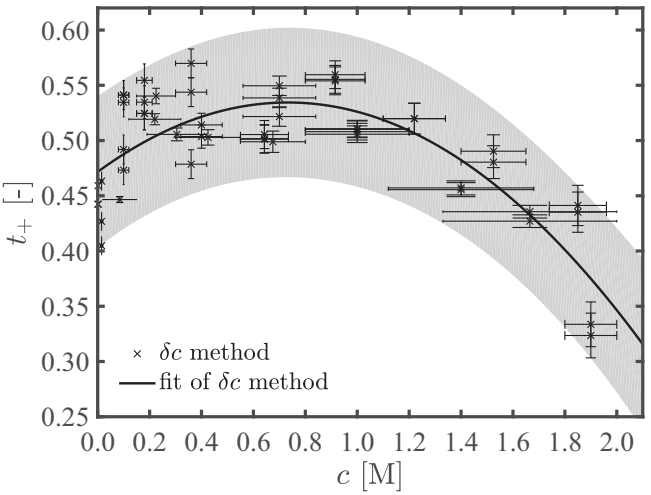

Figure 10. Concentration dependence of the transference number via the δc method, i.e., determined by Eq. 38 from concentration cell data based on small concentration variations ($c_0 \pm \delta c$) and from the concentration dependent thermodynamic factor obtained by ferrocene cell measurements (from Figure 9 in Ref. 2). Vertical error bars represent the effect of the 0.3 mV error of the concentration cell measurements, while the horizontal error bars indicate the experimentally chosen concentration variation δc. The black solid line is a quadratic fit (see Eq. 39) of all the depicted $t_+(c_0 \pm \delta c)$ data and the gray region indicates the 95% confidence interval. The electrolyte used is $LiClO_4$ in EC:DEC (1:1 w:w) and measurements are done inside a temperature controlled glove box.

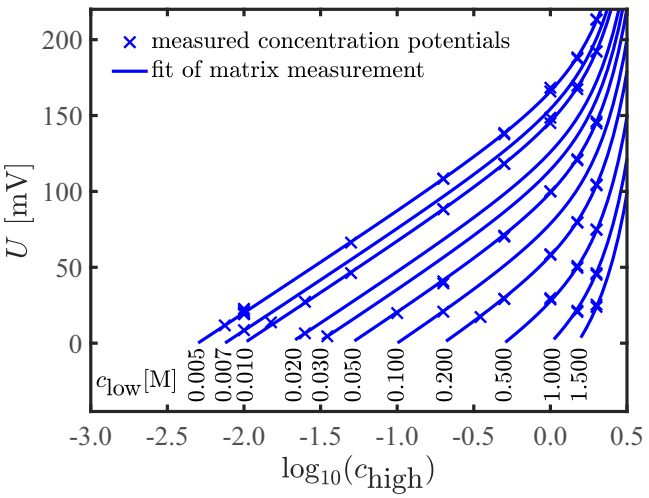

Figure 11. Concentration overpotentials U resulting from a set of permutations of low (c_{low}) and high (c_{high}) salt concentrations measured in the concentration cell setup (see Figure 1). Lower concentrations are indicated below the fit lines inside the figure, while higher concentrations are plotted logarithmically (base 10) on the x-axis. The electrolyte used is $LiClO_4$ in EC:DEC (1:1 w:w) and measurements are done inside a temperature controlled glove box. The solid lines are a numerical fit to Eq. 28.

determined with the δc method is used and shown for comparison. These data will be compared to the literature later on.

Transference number via polarization cell and concentration cell experiments.—In the following, the procedure for the determination of the concentration dependent transference number $t_+(c)$ based on polarization experiments in combination with concentration cell measurements, as outlined in the section Determination of the transference number based on the Sand equation, a concentration cell, and a known diffusion coefficient is investigated. The binary diffusion coefficient $D_\pm(c)$ is obtained from polarization cell experiments in symmetrical Li-Li cells as discussed in Ehrl et al.[1] The factors $f_1(f_\pm,\ t_+,\ D^{*}_{\pm,\ \mathrm{eff}}{}^{0.5})$ or $f_2(f_\pm,\ t_+,\ D^{*}_{\pm,\ \mathrm{eff}})$ given in Eqs. 25 and 29, respectively, are obtained by experiments in a polarization cell using the various methods discussed in the sections Sand equation and Alternative methods for the determination of the transference number (summarized in Table I). The factor $\left[1+\frac{\partial \ln f_\pm(\mathrm{c})}{\partial \ln c}\right](1-t_+(\mathrm{c}))$ (see Eq. 28) is determined from concentration cell experiments in form of a continuous functional description. This will be described in the following.

The required concentration overpotential data were measured in a concentration cell as described in the Experimental section, with exemplary results shown in Figure 9. To be able to extract the factor $\left[1+\frac{\partial \ln f_\pm(\mathrm{c})}{\partial \ln c}\right](1-t_+(\mathrm{c}))$, a set of concentration cell experiments was conducted (over 70 concentration cells were measured, of which most combinations were conducted at least twice). Figure 11 shows the recorded concentration cell potentials U for different lower salt concentrations c_{low} versus the higher salt concentration c_{high}, whereby each line corresponds to a fixed value of c_{low}.

The solid lines in Figure 11 represent the numerical fit of the measured concentration cell potentials using Eq. 28. As a result of the integral in Eq. 28, a functional description has to be assumed a priori for the factor $\left[1+\frac{\partial \ln f_\pm(\mathrm{c})}{\partial \ln c}\right](1-t_+(\mathrm{c}))$. It is found that a third order polynomial represents the experimental data best, polynomials with a lower order result in a poor representation of measured data, while higher order polynomials improve the fit quality only insignificantly and may result in numerical oscillations. The solid lines in Figure 11 thus represent an overall third order polynomial fit of the concentration cell data with the following numerical result

$$\left[1+\frac{\partial \ln f_\pm(\mathrm{c})}{\partial \ln c}\right](1-t_+(\mathrm{c})) = 0.105\,c^3 + 0.042\,c^2 + 0.205\,c + 0.557 \qquad [40]$$

Based on this numerical fit, the transference number at infinite dilution is $t_+(\mathrm{c}\to 0) = 0.44$, since the thermodynamic factor (i.e., the left-hand-term in square brackets) under these conditions approaches unity. This is in good accordance with the the δc method, which yields $t_+(\mathrm{c}\to 0) = 0.47$ (see Figure 10 and Eq. 39). The factors $f_1(f_\pm,\ t_+,\ D^{*}_{\pm,\ \mathrm{eff}}{}^{0.5})$ or $f_2(f_\pm,\ t_+,\ D^{*}_{\pm,\ \mathrm{eff}})$ are determined based on experiments in a polarization cell. As presented in the section Numerical validation, five different analytical expressions based on pulse and steady-state experiments are considered for the determination of $f_1(f_\pm,\ t_+,\ D^{*}_{\pm,\ \mathrm{eff}}{}^{0.5})$ or $f_2(f_\pm,\ t_+,\ D^{*}_{\pm,\ \mathrm{eff}})$. The analytical expressions for these five methods are summarized in Table I and their accuracy was demonstrated by means of numerical simulations in the section Validation of the different parameter determination methods. In the following, the experimentally determined transients are shown exemplarily for the salt concentrations 0.01 M, 0.5 M, 1.5 M, and 2 M. Analysis of the high frequency resistance showed a steady decrease for the 0.01 M electrolyte over the course of the experiments, which we ascribe to side reactions which alter the electrolyte composition (mostly via continuous SEI formation caused by reaction with the freshly plated lithium during the polarization phase). In conclusion, because all factors in Table I depend on the initial salt concentration c_0, the recorded transients for the nominally 0.01 M electrolytes are only shown for the benefit of the reader and are not analyzed for their transference number in the case of polarization cell experiments. Physical vibrations, e.g. from glove box or temperature chambers, play negligible role as a porous medium rather than a free liquid electrolyte is used in the experimental setup. Gas generation is limited due to the small surface area of the lithium electrodes and at ambient temperatures, electrolyte evaporation plays no role in the tight two electrode cells and is negligible over the time of the transference number measurements (vapor pressure of linear carbonates <50 mbar). First of all, the factor $f_1(f_\pm,\ t_+,\ D^{*}_{\pm,\ \mathrm{eff}}{}^{0.5})$ can be determined from pulse experiments based on the Sand equation given in Eq. 26, which requires only the cell potential $U(\tau_\mathrm{I})$ at current interruption time. The accuracy of the method is improved by the observation of the short term relaxation

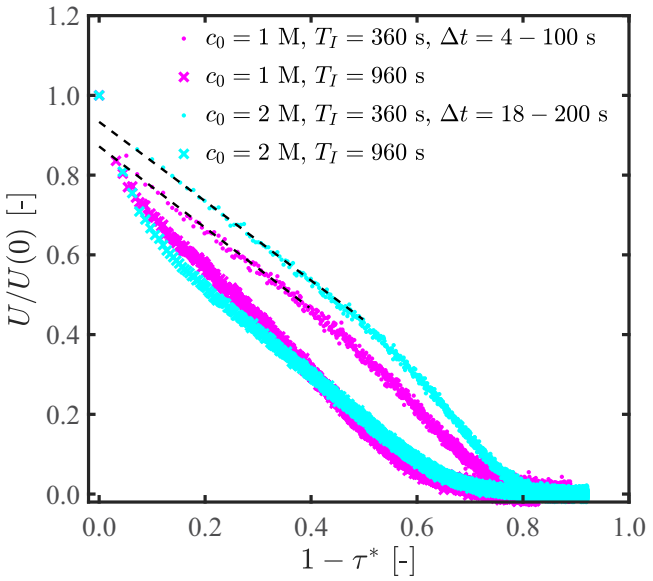

Figure 12. Exemplary relaxation after a current pulse of $i_p = 0.5$ mA (0.22 mA/cm^2) for T_1 values of 360 s or 960 s in either 1.0 M or 2.0 M $LiClO_4$ in EC:DEC (1:1 w:w). This was measured in the two-electrode setup shown in Figure 1 of Ref. 1.

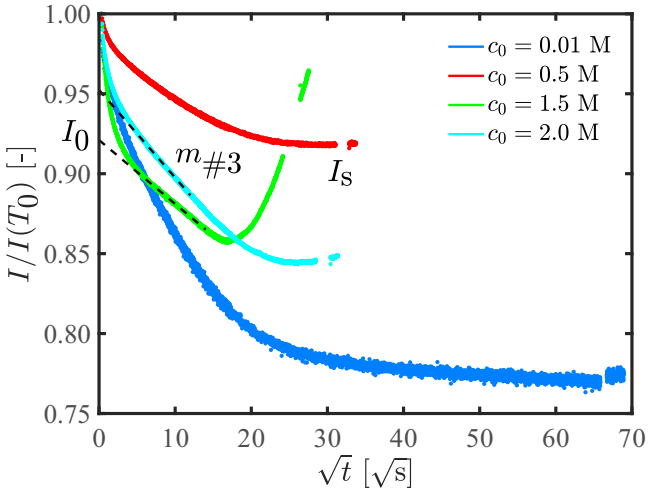

Figure 13. Exemplary steady state polarization current transients for 0.01 M, 0.5 M, 1.5 M, and 2.0 M $LiClO_4$ in EC:DEC (1:1 w:w) at constant polarization of 50 mV in the two-electrode cell shown in Figure 1. The gaps in the curves toward the end of the potentiostatic polarization procedure are due to impedance measurements which were conducted during that time.

after current interruption, which exhibits a linear relationship with respect to the artificial time τ^* defined in Eq. 27. In Figure 12, four normalized potential transients (two different $LiClO_4$ concentrations and interruption times) are depicted vs. the artificial time $1 - \tau^*$. The relaxation curves resulting from the shorter polarization time of $T_1 =$ 360 s (dots in Figure 12) exhibit the theoretically expected s-shape, which can also be observed in the numerical simulations, compare for example the green line in Figure 8a. The linear fits indicated by the dashed black lines correspond to real times between ≈10–150 s. The extrapolations of these fits to $(1 - \tau^*) = 0$ gives the desired cell potential $U(T_1)$ at current interruption time. While a linear relaxation behavior can also be observed for the longer polarization time of $T_1 =$ 960 s (crosses in Figure 12), the typical s-shape as depicted in Figure 8a is missing. This is an indication for a violation of the semi-infinite diffusion boundary condition resulting from too long polarization times, as discussed in the section Influence of the polarization time on the determined transference number in a pulse experiment. However, further reduction of the polarization time decreases the signal to noise ratio and is thus unsuitable for a precise determination of the cell potential at the polarization interruption time. The time transients for all potential relaxation curves in Figure 12 with respect to $\sqrt{(t - T_1)}$ show a non-linear behavior (data not shown), similar to the green line in Figure 8b, which may be caused by the higher sensitivity of the potential relaxation transient with $\sqrt{(t - T_1)}$ toward distortions from, e.g., SEI recreation effects and thus prohibit the dismissal of pulse polarization data. Thus the observation of the S-shape in Figure 12 is considered the best identifier for usability of experimental data and the factor $f_1(f_\pm, t_+, D^*_{\pm,\,\mathrm{eff}}{}^{0.5})|^{\text{pulse polarization}}_{\text{short−term relax.}}$ (method #1) is only analyzed for pulses showing this shape, i.e., pulses of 360 s at 0.5 mA (0.22 mA/cm^2).

All other methods for the determination of the factors $f_1(f_\pm, t_+, D^*_{\pm,\,\mathrm{eff}}{}^{0.5})$ and $f_2(f_\pm, t_+, D^*_{\pm,\,\mathrm{eff}})$ are based on steady-state experiments. At first, the transient behavior of the current $I(t)$ during the potentiostatic polarization at U_p is analyzed. Exemplary current transients for a 0.01 M, 0.5 M, 1.5 M and a 2 M salt concentration are depicted in Figure 13.

While an initial linear current relaxation with respect to time $\sqrt{t}$ can be observed for salt concentrations 1.5 M (green) and 2 M (light blue) as is predicted by Eq. 21, this linearity is not apparent for the 0.01 M (dark blue) and the 0.5 M (red) electrolyte. This cannot be explained by the approximation of the term $\exp(H^2 t)(1 - \mathrm{erf}(H\sqrt{t}))$ with $\sqrt{t}$ as outlined in the theoretical part, since the values for H are of the same order for the depicted concentrations. However, since the theoretical relation between the current and $\sqrt{t}$ is derived based on the linearized Butler-Volmer law and therefore on a constant interface resistance, the observed curvature may result from parasitic effects, which may lead to the sometimes observed decrease of the total charge transfer resistance during the polarization time. The distinct drop of the current in the beginning of the polarization time may also be related to this effect. For larger concentrations, this effect may be restricted to a short time period in the beginning of the polarization, whereas it is distributed over a longer time period for the concentrations 0.01 M and 0.5 M, thereby interfering with the expected $\sqrt{t}$ relaxation. Extrapolation of the linear region in Figure 13 allows for the determination of the initial current I_0. As a result of Figure 13, the factor $f_1(f_\pm, t_+, D^*_{\pm,\,\mathrm{eff}}{}^{0.5})|^{\text{ss polarization}}_{\text{short−term pol.}}$ (method #3, see Table I) is determined only for concentrations $c_0 \geq 1$ M by means of Eq. 32. In this case, the ratio $m_{\#3}/I_0$ is determined based on the linear fits indicated by the black dashed lines in Figure 13. Additionally, the required low frequency resistance $R_{\mathrm{LF},0}$ is measured by impedance spectroscopy before each steady-state experiment.

While for this latter method, it is not necessary that a steady-state is reached at the end of the polarization period, for the remaining three factors $f_2(f_\pm, t_+, D^*_{\pm,\mathrm{eff}})|^{\text{ss polarization}}_{\text{short−term relax.}}$ (method #4), $f_2(f_\pm, t_+, D^*_{\pm,\mathrm{eff}})|^{\text{sss polarization}}_{\text{long−term relax.}}$ (method #5), and $f_2(f_\pm, t_+, D^*_{\pm,\mathrm{eff}})|^{\text{ss polarization}}_{\text{transition period}}$ (method #2), a linear, steady-state current concentration profile is strictly required at the end of the polarization time, as discussed in the section Influence of a non steady-state concentration profile on the determination of the transference number. In a steady-state experiment, the steady-state is indicated by a distinct current plateau at the end of the polarization phase, which is observed for the 0.01 M, 0.5 M, 1 M (data not shown), and 2.0 M electrolytes (see Figure 13). A anomalous time dependence of the current at the end of the polarization phase as depicted, e.g., for $c_0 =$ 1.5 M in Figure 13 (green line) excludes this experiment from analysis based on methods #2, #3, and #5, because a linear concentration profile may not be present at the end of the polarization phase. The increase in the current may be explained by a decreasing interface resistance as a result of a modification of the lithium electrode/electrolyte interface (supported by the fact that the electrolyte resistance remains essentially unchanged over the time of polarization). The factor $f_2(f_\pm, t_+, D^*_{\pm,\mathrm{eff}})|^{\text{ss polarization}}_{\text{transition period}}$ (method #2) defined

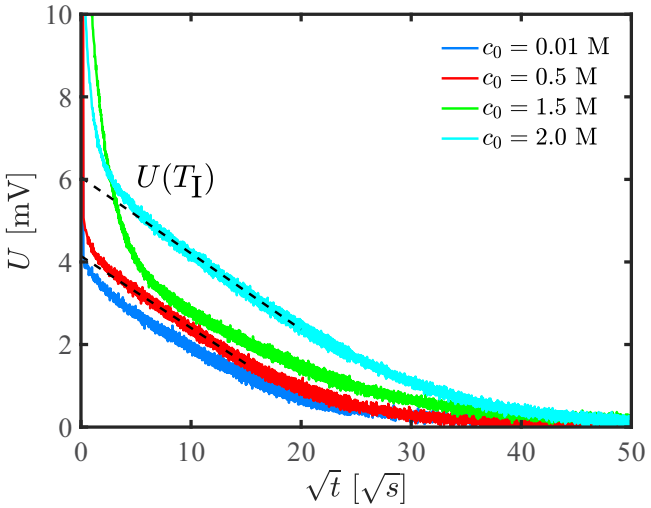

Figure 14. Exemplary fit of time behavior after 50 mV steady-state polarization for determination of the factor $f_2(f_\pm,\ t_+,\ D^*_{\pm,\mathrm{eff}})|^{\text{ss polarization}}_{\text{short−term relax.}}$ (method #4) for 0.01 M, 0.5 M, 1.5 M and 2.0 M $LiClO_4$ in EC:DEC (1:1 w:w) in a polarization cell. Dashed lines indicate linear fits used for determination of the transference number. The polarization times for the different concentrations can be found in the caption of Figure 13.

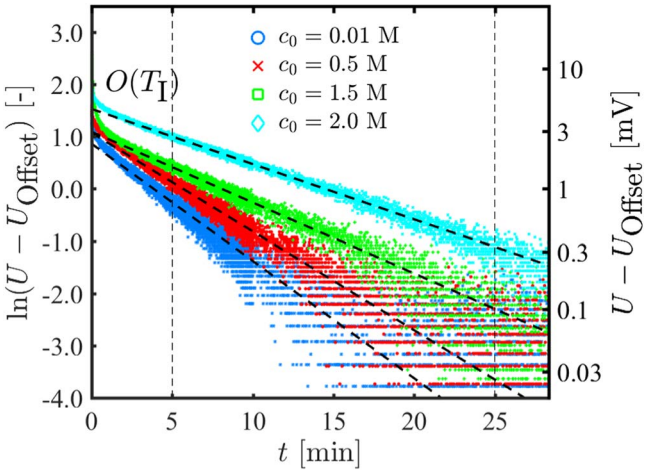

Figure 15. Exemplary fit of the logarithm of the potential vs. time during the relaxation phase after steady-state polarization (50 mV), from which the factor $f_2(f_\pm,\ t_+,\ D^*_{\pm,\mathrm{eff}})|^{\text{ss polarization}}_{\text{long−term relax.}}$ (method #5) can be determined for 0.01 M, 0.5 M, 1.5 M and 2.0 M $LiClO_4$ in EC:DEC (1:1 w:w) in two-electrode cells.

by Eq. 31 is based on the steady state current I_S and the low frequency resistance $R_\mathrm{LF,S}$ at steady state which is determined by impedance spectroscopy at the end of the polarization time. The required steady state current I_s can be extracted from Figure 13. The short period with a constant steady state current in this figure is the result of the scaling with $\sqrt{t}$. The second factor $f_2(f_\pm,\ t_+,\ D^*_{\pm,\mathrm{eff}})|^{\text{ss polarization}}_{\text{short−term relax.}}$ (method #4) is based on the analytical solution for a steady state concentration profile at the end of the polarization phase. In this case, the cell potential $U(T_\mathrm{I})$ at current interruption time and the steady state current I_s has to be determined experimentally to calculate the factor by means of Eq. 34. As it was the case for the determination of the factor $f_1(f_\pm,\ t_+,\ D^{*\ 0.5}_{\pm,\ \mathrm{eff}})|^{\text{pulse polarization}}_{\text{short−term relax.}}$ (method #1), the short-term relaxation behavior of the cell potential can be used to extrapolate the exact cell potential $U(T_\mathrm{I})$ at the time of the potential interruption.

As shown in Figure 14, the expected linear relation with respect to $\sqrt{t}$ can be observed for $c_0 =$ 0.5 M and $c_0 =$ 2 M. On the other hand, the non-linear behavior with respect to $\sqrt{t}$ is a sign for experimental data either with dominating parasitic effects (side reactions in case of the 0.01 M electrolyte) or with instationary concentration profiles at the end of the polarization (as seen in Figure 13 for an initial salt concentration of 1.5 M). As a result, such experimental data are not used for the determination of the factor $f_2(f_\pm,\ t_+,\ D^*_{\pm,\mathrm{eff}})|^{\text{ss polarization}}_{\text{short−term relax.}}$ (method #4). In a steady-state experiment, also the factor $f_2(f_\pm,\ t_+,\ D^*_{\pm,\mathrm{eff}})|^{\text{ss polarization}}_{\text{long−term relax.}}$ (method #5) can be determined from the long-term relaxation behavior by means of Eq. 37. In this context, a linear fit of $\ln U(t)$ with respect to the time t is required, as it is shown for a steady-state experiment in Figure 15 and which can be observed for the relaxation phases for all concentrations investigated. This linear behavior of $\ln U(t)$ with respect to time does not depend on a steady-state profile as it is discussed in part I of this publication (Ref. 1). However, for the determination the transference number a steady-state profile is strictly required which means that although these linear trends are clearly visible in Figure 15 the corresponding relaxation periods cannot be used to calculate the transference number as side reactions (for the 0.01 M electrolyte) or instationary concentration profiles (as clearly visible in Figure 13) violate the theoretical assumptions (see Alternative methods for the determination of the transference number). The offset $O(T_1)$ of such a linear fit is the basis for the determination of the factor $f_2(f_\pm,\ t_+,\ D^*_{\pm,\mathrm{eff}})|^{\text{ss polarization}}_{\text{long−term relax.}}$.

In Figure 16, the transference numbers calculated from polarization experiments using the diffusion coefficient from the first part of this publication[1] are shown and compared to the transference number based on the δc method. Error bars indicate the variation between repeat experiments as well as the error of the diffusion coefficient. A qualitative agreement can be found when comparing the transference numbers determined by the δc method and the methods #1 (black), #3 (red), #4 (magenta) and #5 (green) utilizing the polarization cell. The only outlier is the transference number calculated from the factor $f_2(f_\pm,\ t_+,\ D^*_{\pm,\mathrm{eff}})|^{\text{ss polarization}}_{\text{transition period}}$ (method #2, magenta symbols/line in Figure 16), which is based on the polarization phase of a steady-state experiment. In this case, the qualitative behavior is in accordance with the other methods, but the absolute value is

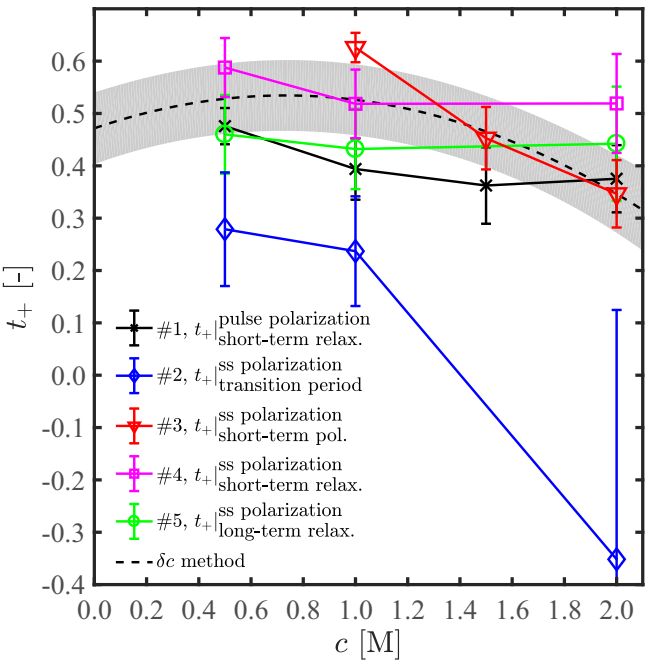

Figure 16. Overview and comparison of transference numbers determined from polarization experiments via factors summarized in Table I and comparison with transference numbers obtained from the δc method (see Figure 10).

significantly smaller, especially at higher concentrations. Unfortunately, there is no obvious reason for this behavior. For 10 mM concentrations, the electrolyte resistance measured in polarization cells by impedance spectroscopy is not constant over the entire experiment. No final assignment of latter effect was possible which is why polarization cell data with 0.01 M salt concentrations could only be used for the determination of concentration independent transport factors; at these low concentrations, only the diffusion coefficient could be determined, as shown in the first part of this study.[1] Thus, the only reliable method for the determination of the transference number at low concentrations is the δc method, as it requires no current flow at the lithium electrodes and thereby minimizes the effect of side reactions.

Although the qualitative results of the transference number determined by polarization experiments are comparable to the transference number determined by the δc method in a concentration cell, the method based on data from a concentration cell is clearly superior. It is much easier to perform experiments in the concentration cell than in the two-electrode cell. Another advantage of the concentration cell is that only the concentration overpotential resulting from two differently concentrated electrolyte solutions is measured. Therefore, additional physical phenomena such as mass and current transport do not influence the results. Also, the number of required experiments is reduced from three to two experiments, resulting in a decreased number of potential error sources. A similar result as shown in Figure 16 is obtained when the transference number is determined based on a known thermodynamic factor and polarization cell experiments (data not shown), rather than using the data from concentration cells (i.e., the data shown in Figure 11).

Although the direct determination of the transference number introduced in the section Direct determination of the transference number by steady-state polarization experiments has initially been developed for polymer electrolytes, it is also often applied for liquid electrolytes,[28–30] ionic liquids[31] or mixtures of both,[32] even though it strictly is valid only for dilute solutions and cannot be applied to concentrated solutions due to a violation of the underlying assumptions as indicated in the section Direct determination of the transference number by steady-state polarization experiments. It is also shown that the experimental setup of the polarization cell with two lithium metal electrodes and the $LiClO_4$ electrolyte, as used in this contribution, is not suitable for low salt concentrations, since a constant electrolyte resistance cannot be guaranteed. However, a constant electrolyte resistance is the basic requirement for the direct determination of the transference number.

Comparison with the literature.—In the literature a wide variety of transference numbers of liquid non-aqueous electrolytes is reported which are collected for similar electrolyte systems in Figure 17. Basically constant transference numbers of ∼0.4 for $LiPF_6$ in a PC/EC/DMC mixture E(10:27:63 v:v:v, red squares),[5] of ∼0.42 for LiTFSI in PC (green pluses),[14] or of ∼0.45 for LiDFOB in EC:DEC (3:7 w:w, magenta triangles)[9] are reported in the literature. While in all these reports, in which the transference number does not change more than 10% in the investigated concentration range, the salts and solvents differ, also strong concentration dependencies are reported for example for $LiPF_6$ electrolytes. Monotonically decreasing values for the lithium transference number are reported by Nyman et al.[19] for $LiPF_6$ in EC:EMC (3:7 w:w, red crosses) and Lundgren et al.[20] for $LiPF_6$ in EC:DEC (1:1 w:w, red diamonds). While comparison of the reports for $LiPF_6$ based electrolytes (compare red symbols in Figure 17) show the influence of the solvent on the transference number, direct comparison with the electrolyte investigated in this work is difficult due to the different salts, solvents, and measurement techniques. Although the only reference depicted in Figure 17 using $LiClO_4$ salt uses PC as solvent (blue stars),[18] it is closest to our electrolyte composition ($LiClO_4$ in EC:DEC, 1:1 w:w, black line) and to the authors best knowledge, no literature is available investigating exactly the same electrolyte as used in this work. In the latter publication the authors also use a second order polynomial to describe the concentration dependence of the transference number resulting in a similar behavior compared to our results, only shifted to smaller values.

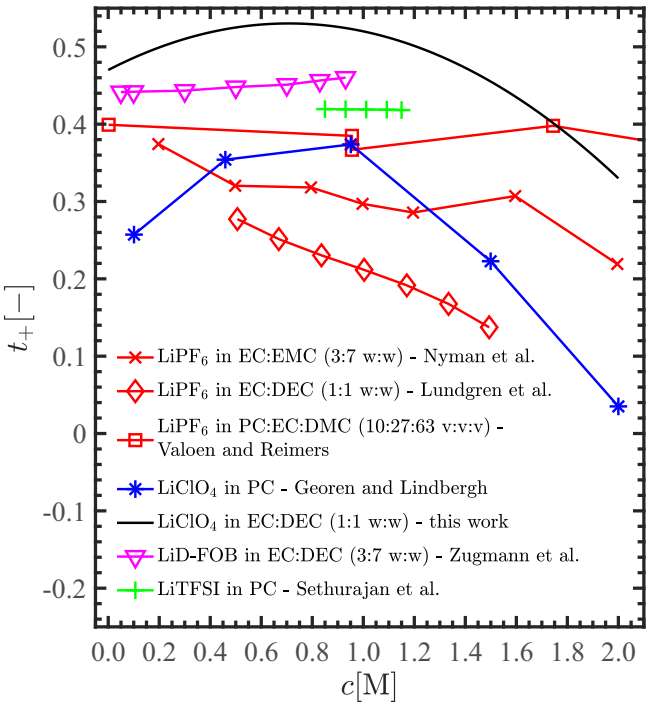

Figure 17. Literature comparison of transference numbers for a range of electrolytes: $LiPF_6$ in EC:EMC (3:7 w:w) - Nyman et al.,[19] $LiPF_6$ in EC:DEC (1:1 w:w) - Lundgren et al.,[20] $LiPF_6$ in PC:EC:DMC (10:27:63 v:v:v) Valøen et al.,[5] $LiClO_4$ in PC - Georén and Lindbergh,[18] $LiClO_4$ in EC:DEC (1:1 w:w) – this work, LiD-FOB in EC:DEC (3:7 w:w) - Zugmann et al.[9] and LiTFSI in PC - Sethurajan et al.[14]

At low concentrations the transference number is defined by ion-solvent interactions, i.e., different mobility of anions and cations with their respective solvation shell within an excess of solvent molecules, and thus we expect different values for different solvent-salt combinations. In conclusion, the largely constant offset of ∼0.2 of the transference numbers for $LiClO_4$ in PC compared to EC:DEC (1:1 w:w) may be ascribed to the effect of the solvent. At concentrations above ∼0.8 M the transference number of the $LiClO_4$ electrolytes decreases (compare blue stars and black line in Figure 17). A decreasing transference number with an increasing salt concentration is explained by the formation of ion-pairs in the literature.[14,15] A similar effect was previously reported by Vatamanu et al.[33] Another explanation for the decrease of the transference number might be related to the ratio of moles of solvent to moles of salt. Depending on the solvation structure of the salt ions, a large fraction of the solvent (predominantly EC or PC) may be bound in the solvation shells around the ions. In consequence, the loosely solvated ion, generally the anion due to its large size to charge ratio, may still move mostly undisturbed through the electrolyte at high concentrations (small solvent to salt molar ratio) while movement of the strongly solvated cation is hindered by its solvation shell which includes an increasingly large fraction of the entire electrolyte. In the limiting case of very high molar ratios of salt/solvent, the cations may have to drag along the entire solvent (bound to its solvation shell), so that their mobility will decrease strongly compared to the anions, corresponding to a decrease of the cation transference number at high concentrations. The increase of the transference number, as evident from the $LiClO_4$ electrolytes for concentrations up to ∼0.8 M (compare blue stars and black line in Figure 17), may be explained by the coupled movement of ions at medium concentrations, while at high concentrations the effects of the solvation structure dominate.

Conclusions

In this work, a novel approach for the determination of the transference number is proposed. As a result of the direct determination of the thermodynamic factor introduced in Landesfeind et al.,[2] the transference number can be calculated based on data from concentration cells. The proposed procedure referred to as the δc method is based on small concentration variations and does not require a functional description for the concentration dependence of the transference number.

In addition to the determination via the concentration cell, the transference number is also determined by the classical experimental approach based on a known binary diffusion coefficient and data from polarization cell and concentration cell experiments. This work discusses five different experimental methods for the determination of the transference number based on polarization cell experiments, whereas three of the five methods have not yet been used in the literature for the determination of the transference number. These latter new methods are based on the initial relaxation behavior of the current in a potentiostatic polarization experiment and on the short-term and the long-term relaxation behavior of the cell potential after a potentiostatic polarization experiment. The basic principle of all electrochemical pulse experiments, the validity of the proposed methods as well as chances and potential risks are analyzed by numerical simulations.

In the end, experimental results of all discussed methods, obtained with an exemplary electrolyte solution ($LiClO_4$ in EC:DEC, 1:1 w:w) are compared. Resulting transference numbers based on polarization cell experiments and the δc method generally agree, however, experimental efforts and uncertainties are much higher in the approaches based on polarization cell experiments, since they require to combine results of three different experimental procedures. For a simple and accurate determination of the transference number, measurements of the thermodynamic factor in a ferrocene cell in combination with concentration cell data are superior to polarization cell experiments. It is also shown that the direct determination of the transference number by a steady-state potentiostatic polarization step is not suitable for concentrated binary electrolyte solutions.

List of Symbols

Symbol	Name	Unit
A	electrode area	cm^2
c	ionic concentration	mol/L
D_i	diffusion coefficient	cm^2/s
F	Faraday constant	C/mol
f_1	factor defined by Eq. 25	$\sqrt{s/cm^2}$
f_2	factor defined by Eq. 29	s/cm^2
$f_\pm$	mean molar activity coefficient	-
i_i	current density	mA/cm^2
I	current	A
l	distance between electrodes	µm
$m_{\ln}$	slopes of $\ln U$ vs. t during relax. after steady state pot. pol.	1/s
$m_{\#3}$	slope of $I(t)$ vs. $\sqrt{t}$ during steady state pot. pol.	$A/\sqrt{s}$
$m_{\#4}$	slope of $U(t)$ vs. $\sqrt{t}$ during relax. after steady state pot. pol.	$V/\sqrt{s}$
O	constant factor in Eq. 36	-
R	gas constant	J/(mol K)
$R_{el,i}$	electrolyte resistance	Ω
$R_{LF,i}$	resistance	Ω
t	time	s
t_i	transference number of lithium ion	-
T	temperature	K
T_I	polarization time	s
TDF	thermodynamic factor	-
U_i	potential	V
ν_i	stoichiometry factor	-
x	space coordinate	µm
z_i	ionic charge	-

Greek

κ	conductivity	mS/cm
$\Delta\Phi$	difference of the volumetric intrinsic phase average of the electric potential	V
τ	tortuosity	-
ε	porosity	-
Δc	concentration diff. betw. electrodes	mol/L
τ^*	artificial time	-

Subscripts and Superscripts

Symbol	Name
A	anode
C	cathode
eff.	effective value of parameter with $x_{\text{eff.}} = \frac{\varepsilon}{\tau}\ x$
high	higher concentration in concentration cell
low	lower concentration in concentration cell
p	during polarization
s	steady state
0	initial state
+	cation
−	anion
±	of binary electrolyte

Acknowledgment

We gratefully acknowledge the funding by the Bavarian Ministry of Economic Affairs and Media, Energy, and Technology for its financial support under the auspices of the EEBatt project.

References

1. A. Ehrl, J. Landesfeind, W. A. Wall, and H. A. Gasteiger, *J. Electrochem. Soc.*, **164**, A826 (2017).
2. J. Landesfeind, A. Ehrl, M. Graf, W. A. Wall, and H. A. Gasteiger, *J. Electrochem. Soc.*, **163**, A1254 (2016).
3. J. Newman and K. Thomas-Alyea, *Electrochemical Systems*, 3rd ed., Wiley Interscience, Hoboken, (2004).
4. P. G. Bruce, M. T. Hardgrave, and C. A. Vincent, *Solid State Ionics*, **53–56**, 1087 (1992).
5. L. O. Valøen and J. N. Reimers, *J. Electrochem. Soc.*, **152**, A882 (2005).
6. P. Bruce and C. Vincent, *J. Electroanal. Chem.*, **225**, 1 (1987).
7. M. M. Hiller, M. Joost, H. J. Gores, S. Passerini, and H.-D. Wiemhöfer, *Electrochim. Acta*, **114**, 21 (2013).
8. V. Mauro, A. Daprano, F. Croce, and M. Salomon, *J. Power Sources*, **141**, 167 (2005).
9. S. Zugmann, M. Fleischmann, M. Amereller, R. M. Gschwind, H. D. Wiemhöfer, and H. J. Gores, *Electrochim. Acta*, **56**, 3926 (2011).
10. M. R. Wright, *An Introduction to Aqueous Electrolyte Solutions*, John Wiley & Sons, Ltd, Chichester, (2007).
11. F. Castiglione, E. Ragg, A. Mele, G. B. Appetecchi, M. Montanino, and S. Passerini, *J. Phys. Chem. Lett.*, **2**, 153 (2011).
12. C. Capiglia, Y. Saito, and H. Kageyama, *J. Power Sources*, **81**, 859 (1999).
13. J. Zhao, L. Wang, X. He, C. Wan, and C. Jiang, *J. Electrochem. Soc.*, **155**, A292 (2008).
14. A. K. Sethurajan, S. Krachkovskiy, I. C. Halalay, G. R. Goward, and B. Protas, *J. Phys. Chem. B*, **119**, 12238 (2015).
15. Y. Ma, M. Doyle, T. F. Fuller, M. M. Doeff, L. C. Jonghe, and J. Newman, *J. Electrochem. Soc.*, **142**, 1859 (1995).
16. A. Ferry, M. Doeff, and L. DeJonghe, *Electrochim. Acta*, **43**, 0 (1998).
17. M. M. Doeff, L. Edman, S. E. Sloop, J. Kerr, and L. C. De Jonghe, *J. Power Sources*, **89**, 227 (2000).
18. P. Georén and G. Lindbergh, *Electrochim. Acta*, **49**, 3497 (2004).
19. A. Nyman, M. Behm, and G. Lindbergh, *Electrochim. Acta*, **53**, 6356 (2008).
20. H. Lundgren, M. Behm, and G. Lindbergh, *J. Electrochem. Soc.*, **162**, 3 (2014).
21. P. Blonsky, D. Shriver, P. Austin, and H. Allcock, *Solid State Ionics*, **18–19**, 258 (1986).
22. C. M. Doyle, *PhD Thesis*, Berkeley (1996).
23. A. Ehrl, *PhD Thesis*, München (2016).
24. J. Landesfeind, J. Hattendorff, A. Ehrl, W. A. Wall, and H. A. Gasteiger, *J. Electrochem. Soc.*, **163**, A1373 (2016).
25. A. J. Bard and L. R. Faulkner, *Electrochemical Methods - Fundamentals and Applications*, 2nd ed., John Wiley & Sons, Inc., New York, (2001).

26. H. Hafezi and J. Newman, *J. Electrochem. Soc.*, **147**, 3036 (2000).
27. W. Polifke and J. Kopitz, *Wärmeübertragung: Grundlagen, analytische und numerische Methoden*, Pearson Deutschland GmbH, (2009).
28. C. L. Berhaut, P. Porion, L. Timperman, G. Schmidt, D. Lemordant, and M. Anouti, *Electrochim. Acta*, **180**, 778 (2015).
29. L. Niedzicki, M. Kasprzyk, K. Kuziak, G. Z. Zukowska, M. Marcinek, W. Wieczorek, and M. Armand, *J. Power Sources*, **196**, 1386 (2011).
30. G. A. Elia, J.-B. Park, Y.-K. Sun, B. Scrosati, and J. Hassoun, *ChemElectroChem*, **1**, 47 (2014).
31. C. Liu, X. Ma, F. Xu, L. Zheng, H. Zhang, W. Feng, X. Huang, M. Armand, J. Nie, H. Chen, and Z. Zhou, *Electrochim. Acta*, **149**, 370 (2014).
32. K. Kimura, J. Hassoun, S. Panero, B. Scrosati, and Y. Tominaga, *Ionics (Kiel)*,, 895 (2015).
33. J. Vatamanu, O. Borodin, and G. D. Smith, *Methodology*, **116**, 1114 (2012).